A LASER DISTANCE MEASURING INSTRUMENT

DRA

A Thesis Presented

by

Thomas George White

to

The Faculty of the Graduate College

of

The University of Vermont

NGL 46-001-008

In Partial Fulfillment of the Requirements

for the Degree of Master of Science

October, 1972

64

Accepted by the Faculty of the Graduate College, the University of Vermont, in partial fulfillment of the requirements for the degree of Master of Science, specializing in Electrical Engineering.

Thesis Committee Ronald W. Williams Advisor
Dr. Ronald W. Williams
David M. Ellis
Wilfred Read
Robert J. Dawson Chairman
Dean, Graduate College

Date May 31, 1972

ABSTRACT

A description of a continuous wave helium-neon gas laser using a beam sweep process in the design of a distance measuring instrument is presented. The various parameters of the system are investigated and optimally selected within the confines specified by the desired system characteristics. A transmitter unit was designed and constructed and the electronics necessary to extract the distance information as received from the transmitter unit was designed and a prototype built. The entire system has been tested and data is given. The results indicate that taking an average of 12 readings at any one distance will give the desired second order accuracy, and that a modification in the electronic circuit will substantially improve the system performance.

ACKNOWLEDGEMENTS

The author wishes to express his gratitude to Dr. Lloyd M. Lambert for the project proposal and initiation; to Dr. Ronald W. Williams who acted as a faculty advisor in Dr. Lambert's absence (sabatical leave); to Dr. David M. Ellis who offered many helpful suggestions throughout the project; to Dr. Robert F. Dawson who provided indispensible advice regarding the Civil Engineering aspects of the problem; and, to the National Aeronautics and Space Administration (NASA Institute Project 71-18) for financial support during the summer '71.

TABLE OF CONTENTS

LIST OF TABLES

LIST OF FIGURES

FIGURE PAGE

LIST OF PLATES

CHAPTER I

INTRODUCTION

There are several manufactures of short-range electronic distance measuring devices on the commercial market. The fundamental principle underlying the design of most of the units available today is either time of flight measurement or phase shift measurements. In the first case, electromagnetic radiation is emitted at one extreme of the distance to be measured, a reflector is placed at the other, and the total time it takes the radiation to transverse this distance is recorded. Knowing the speed of electromagnetic radiation and any factors which may alter this value such as air density (barometric pressure and temperature), it is a simple matter to calculate the distance between the emitter and reflector. $L = ct$, where L = the distance of separation, c = the speed of the radiation, and t = the time elapsed. In the second casd, a known modulation is present on the signal beam and the phase shift upon reflection of the returned beam is recorded. There is a direct linear relationship between the degrees of phase shift and the distance of separation. In both cases, however, it is required that the associated electronic circuitry be rather sophisticated and as a result quite costly.

It is the purpose of this study to investigate the design of a low-cost, accurate, short-range electronic distance measuring device using a continuous wave (cw) helium-neon laser in a beam sweeping mode as opposed to a pulsed or modulated system.

The emitter unit contains the portable HeNe laser and the sweep mechanism; the receiver unit contains the photodetectors and the necessary electronics to process the signal. The two photodetectors are

separated at a fixed distance D, and the beam sweep angular speed w, is held constant. The fundamental range of this instrument is set between 100' and 1000' -- distances normally encountered in everyday short-range surveying.

CHAPTER II

SYSTEM DESIGN

Mathematical Approximations

The basic assumption of this system design is that the distance of separation between the sending and receiving unit is inversely proportional to the pulse interval as determined by the beam sweeping across the two photodetectors. This must be mathematically justified. In order to describe the system, consider the diagram presented in figure 1. In that diagram, w = the angular speed of the sweep mechanism, p = the angle swept, D = the photodetector separation, and L = the distance between the emitter and receiver. As noted from the figure, there is a discrepancy between the separation D and the vertical separation of the points a and b (dotted line). Let one half this distance be g (Figure 2). When L is at its minimum of 100', g is noted to be larger than when L is at its maximum of 1000'. Therefore, only if g is negligible at 100' will this discrepancy be eliminated. From figure 2, it is seen that

$$D/2 = L \sin(p/2) + g,$$

$$h/2 = L \sin(p/4), \text{ (from } L\sin(p/2)=h\cos(p/4))$$

$$d = h \sin(p/4),$$

$$g = r \sin(p/2), \text{ and}$$

$$d = r \cos(p/2).$$

By eliminating d, r, and h from the last four equations we obtain for g:

$$g = 2L \sin^2(p/4) \tan(p/2)$$

$$= 2L \tan(p/2) (\tfrac{1}{2} - \tfrac{1}{2} \cos(p/2))$$

$$= L (\tan(p/2) - \sin(p/2)).$$

Let D be chosen such that at 100' p does not exceed 0.068 radians (4°). Then the tangent and the sine of the angle p/2 are

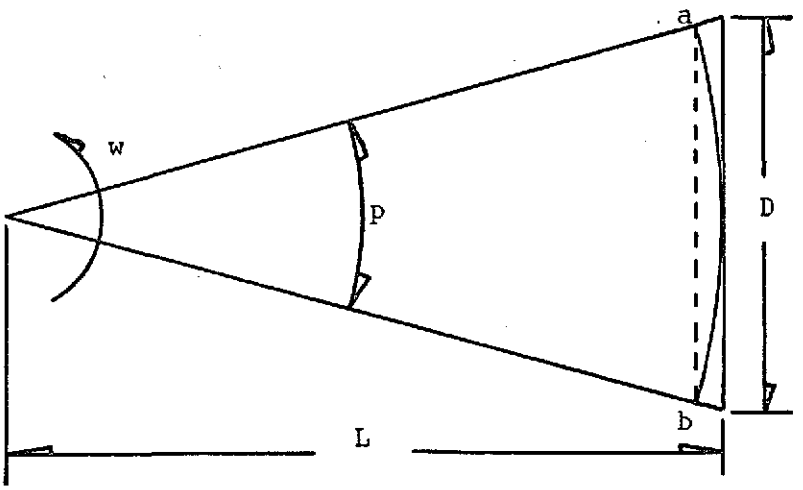

Figure 1. Beam Sweep Schematic

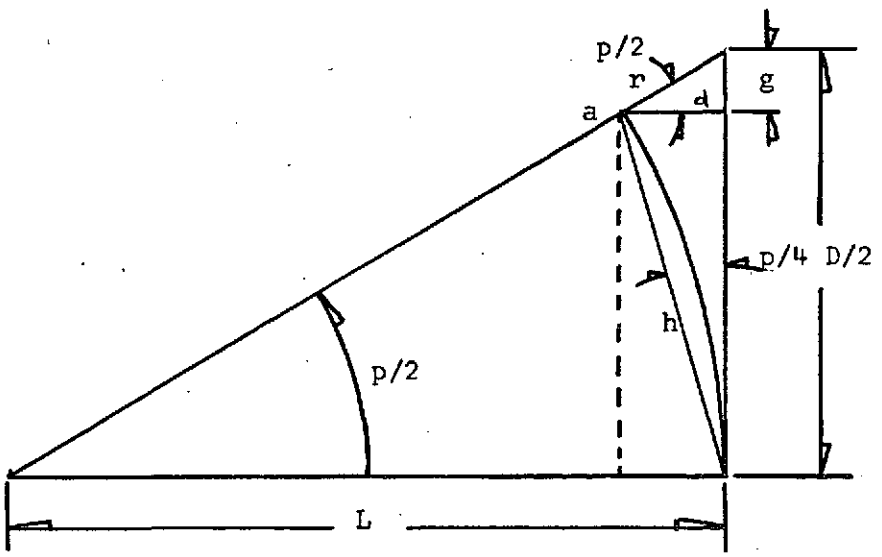

Figure 2. Exaggerated Sketch of the System Geometry

$$\tan(0.034) \doteq 0.03401, \text{ and}$$

$$\sin(0.034) \doteq 0.03399.$$

Hence, g is described by

$$g = 100'(0.00002)$$

$$= 0.002'$$

$$= 0.024".$$

Since the photodetectors to be used have an active junction diameter of 0.49", 0.024" will not cause any significant variation in the time interval as the distance L is increased; ie, as 0.024" approaches 0.000" as L approaches its upper limit.

This being the case, g can be dropped from the equation

$$D/2 = L \sin(p/2) + g,$$

with the results that $D/2 = L \sin(p/2)$.

However, $\sin(0.034) = 0.03399 \doteq 0.034$, so let us therefore assume that in all cases concerned that

$$D/2 = L\,(p/2), \text{ or}$$

$$D = Lp.$$

From figure 1, we observe that $w = p/t$, or $t = p/w$. Since $p = D/L$, we have that $t = D/Lw$. Thus it is seen that with D and w fixed, the time of separation between the two pulses is inversely proportional to L. Let D be selected as 2 pi feet, and the sweep frequency be chosen as 1 Hz. Since $w = 2 \text{ pi } f$, we have that $t = 1/L$ seconds, where L is in feet.

The design problem can be stated as follows: Obtain a beam sweep with w being very constant (in order to retain the validity of the equation $t = 1/L$), record the time t, invert this quanity and display the results.

Range and Necessary Accuracy of the Instrument

The primary consideration of any distance measuring instrument is the range of distances to be measured. Since we are dealing with a short-range instrument, we select a range of between 100' and 1000' as a good working value, the justification being that a good percentage of actual surveying work lies in this range.

The standard deviation of a series of measurements is defined as σ (sigma), such that $$\sigma = \pm \sqrt{\frac{\sum_{i=1}^{n}(x_i - \bar{x})^2}{n-1}},$$ where x_i is a particular measurement, $\bar{x}$ is the mean value, and n is the total number of measurements. The standard deviation is a good figure of merit for any distance measuring instrument. The system design will try to achieve second order accuracies throughout its range which is to say that the measurements should not have errors greater than 1 part per 15,000 (reference 5).

Selection of Beam Sweeper and Laser

The next logical question to ask is what value for the angular speed of the beam sweep mechanism would be optimal? Factors affecting this choice are the dependence of the accuracy of the sweep mechanism on the frequency of rotation, the total time available for each measurement, and the transfer of sufficient energy to the receiver at the upper limit of the distances to be measured.

First of all, a source: Of the available methods, a judicious choice was considered to be the servomotor from the Sony Model TC-800B Tape Recorder. See plates 1 and 2. From all aspects, this motor, due to its large inertia, many magnetic feedback sensors and the disposition

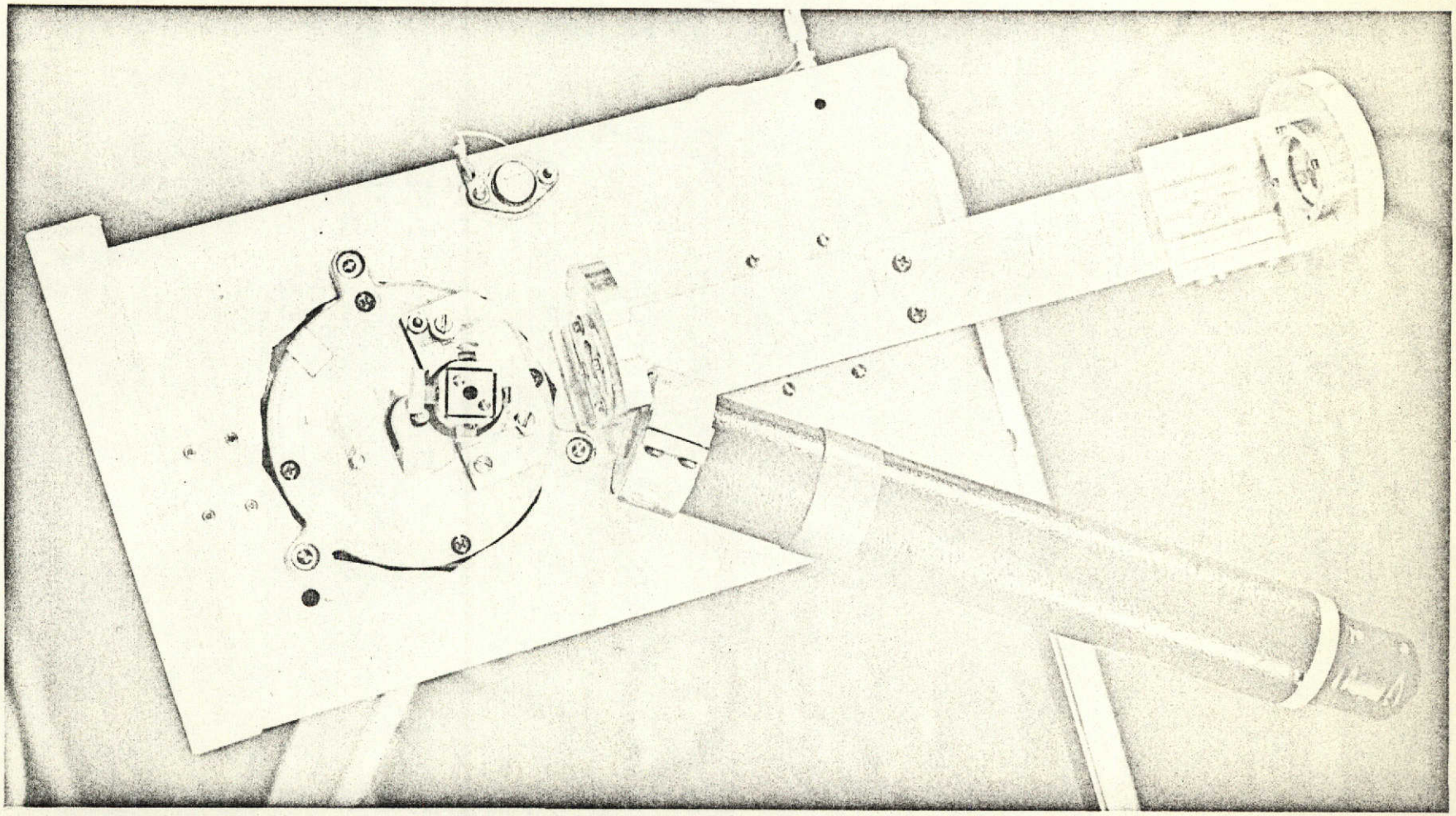

Plate 1. The Beam Sweep Unit: The 0.75 mw Laser, the Servomotor, and the Telescope.

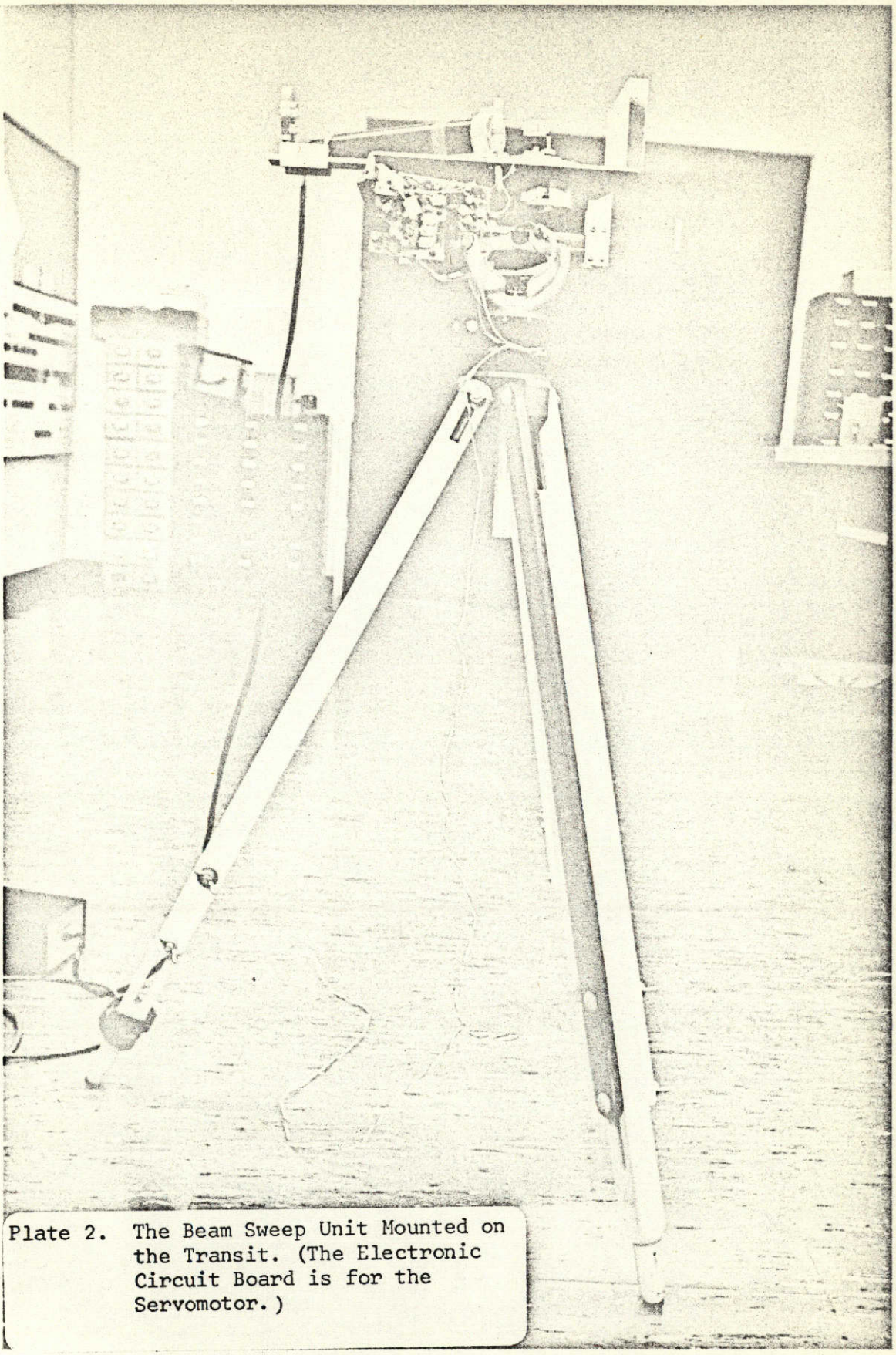

Plate 2. The Beam Sweep Unit Mounted on the Transit. (The Electronic Circuit Board is for the Servomotor.)

of four shaft angular frequencies (1 Hz, 2 Hz, 3 Hz, and 4 Hz) was chosen as being sufficient for the prototype. The actual ability of the motor to retain constancy in angular speed is to be determined from the experimental set-up.

With a load applied to the motor, the most constant angular speed is 4 Hz. The other speeds show a reduced ability to control this constancy of frequency, the 1 Hz resulting the poorest. However, the primary design is to epoxy a front surface mirror on top of the shaft--this is the total load. (Note that on plate 1 there is mounted a cubical structure on a rubber drive wheel with four front surface mirrors epoxied to each face. This was an earlier design which later proved to be inadaquate and hence abandoned for the simpler mirror mounted directly on the shaft.) See Figure 3. Because of its rather large inertia and the state of no load, it will be assumed that even at its lowest frequency of 1 Hz, the servomotor will have sufficient constancy of angular speed, w.

The time available for the measurement to be taken is considered reasonable if it lies in the range of from 5 seconds to 2 minutes. As we shall see later, choosing the 1 Hz source has a direct effect on the time of measurement, but a discussion of this dependence must be posponed until the intricacies of the electronics is considered.

The lowest frequency is desirable from the energy standpoint in that it maximizes the amount of energy transferable to the photodetectors. At 100', the energy transferred is no problem, but at 1000' when the lineam velocity of the beam sweeping past the photodetectors has a magnitude of ten times that at 100', the rational of selecting the lowest frequency is easity appreciated.

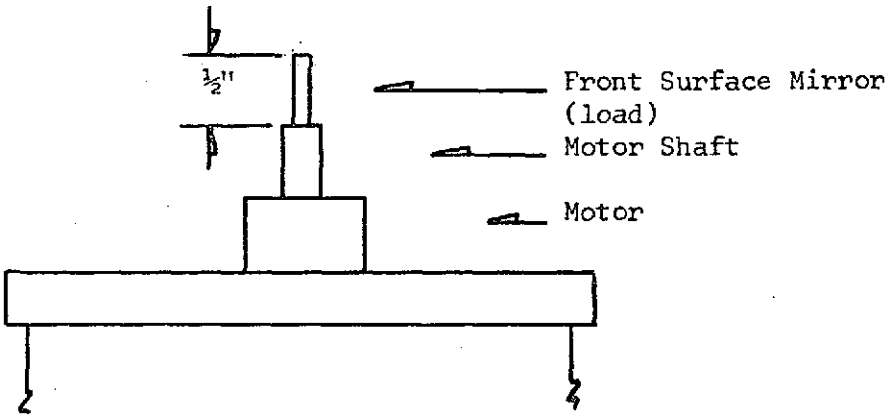

Figure 3. The Front Surface Mirror Mounted on the Shaft of the Servo-motor.

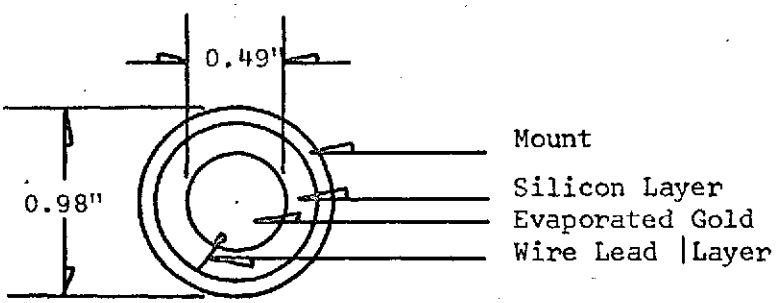

Figure 4. Dimensions of the Schottky Barrier Photodiodes

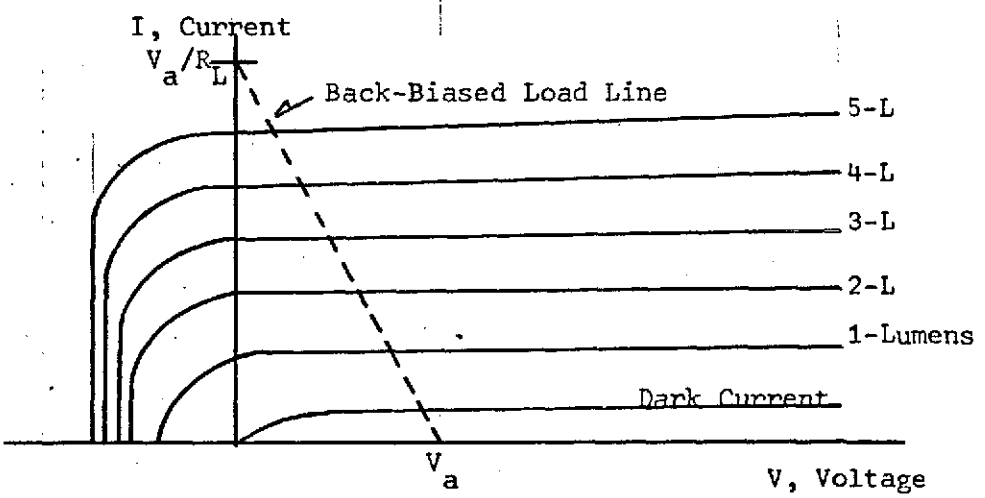

Figure 5. The V-I Characteristic Curves for the Schottky Barrier Photodiodes

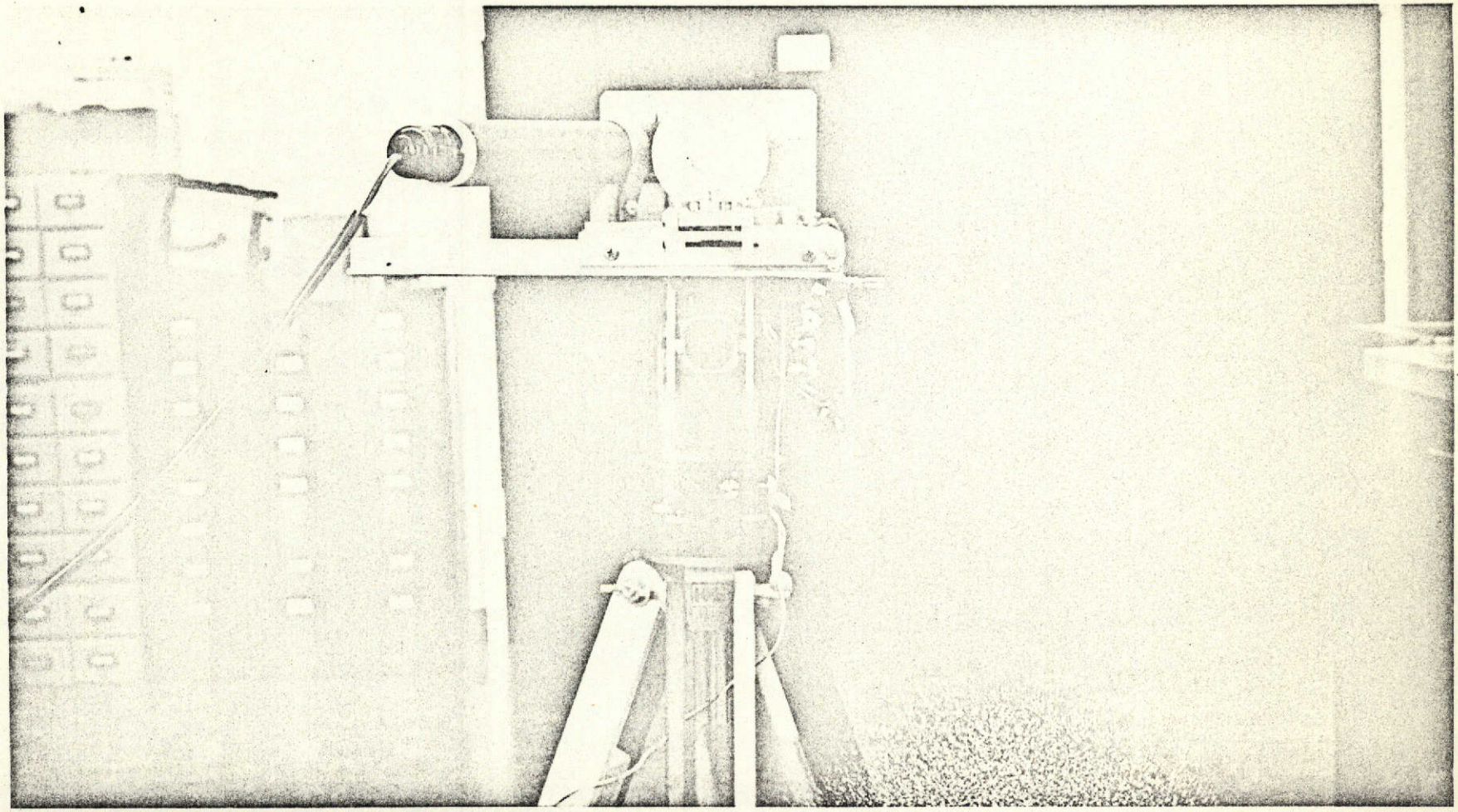

Plate 3. The Sweep Unit with the Laser Beam Directed into the Camara Lens. The Transit Telescope is Aligned Paralled to the Beam.

The laser to be used is a 0.75 mw Helium-Neon cw gas laser. Based on the 1 Hz sweep frequency, energy transfer calculations which shall be done subsequently offer a means of predicting if the 0.75 mw laser has sufficient power for the maximum range of 1000'.

Selection of the Photodiodes and Optical Filter

The photodetectors selected are two United Detector Technology PIN-10 Schottky Barrier Standard Silicon Photodiodes. They have dimensions as depicted in figure 4. A PIN photodiode is one in which a heavily doped p-region is separated by a material which is nearly intrinsic (reference 1). The advantages of the PIN diodes are good response time, responsivity, and linearity. The V-I characteristic curves for the Schottky Barrier diode is shown in figure 5. The photodiodes will operate in the back-biased mode in order to take advantage of the detector's linearity and to decrease the risetime response. The maximum power before saturating is given as 1 mw/cm^2. Since the 0.75 mw laser has a beam area at 100' greater than 1 cm^2, it is obtained that the power density of the laser beam over the complete range is less than 1 mw/cm^2 which implies complete linearity.

The complete spectral response of the photodiodes is from 0.28 microns to 1.07 microns with a minimum absolute responsivity of 0.26 uamps/uwatts at 0.6328 microns, the wavelength of the laser used. The responsivity of a photodiode is a measure of its sensitivity to light and is defined as the ratio of the current produced by the diode (amps) to the amount of light falling on it (watts).

With such a responsivity it would be impossible to detect a swept laser beam of relativity low power without some means of eliminating the unwanted background intensity. Hence, a special optical filter

is used which has a 30 angstrom bandwidth at the center wavelength of 6328 angstroms. The transmission of the filters at the center wavelength is between 70 and 80%. Also, in order to reduce the effects of any spurious incident light, the photodetectors are sheathed in a 3" cylindrical tube (figure 6). The angle of acceptance q, is given by $q = 2 \tan^{-1}(d/2a)$; where d = 0.98", a = 1.5" and, q ≐ 36 degrees. However, since the sweep angle between the photodetector at 100' is just q ≐ 4 degrees (with the photodetector separation at 2 pi feet), there will be no problem as to the beam acceptance.

We now have the beam from the HeNe gas laser being swept at 1 Hz across two filtered photodiodes. The question now remains as to the exact nature of the spatial energy distribution of the beam. For example, consider the unlikely case where the distribution of intensity appears as in figure 7. If this were the case, there would result in two pulses per diode and the system would necessarly have to be designed around this fact.

Spatial Distribution of the Laser Beam

To investigate the nature of the beam shape, consider first the operation of the laser: A gas laser consists of a discharge tube enclosed in a resonant cavity; in this case, the cavity is a hemispherical one, which means that one end has a plane circular dielectric mirror, and the other has a spherically circular dielectric mirror with a radius of curvature equal to the mirror separation. Due to the effect of stimulated emission within the tube, the wavefront is planar and uniform in both amplitude and phase. Therefore, in essence the beam shape upon emergence from the circular mirror is goverened simply by Fraunhofer diffraction at a circular aperature. Following Born and Wolf (reference

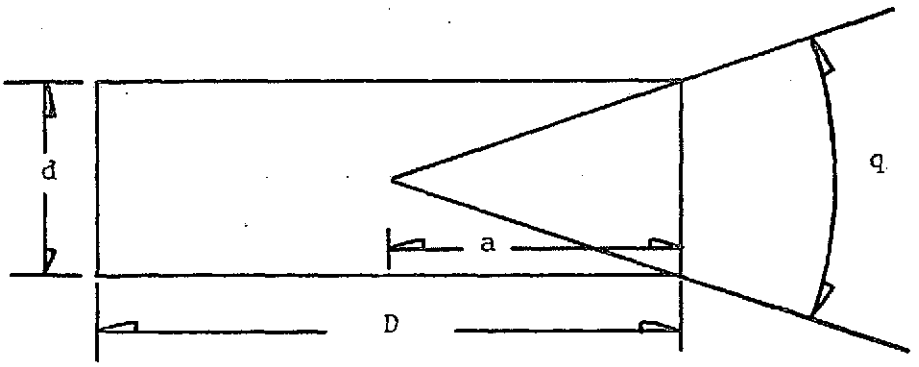

Figure 6. Photodetector Sheath

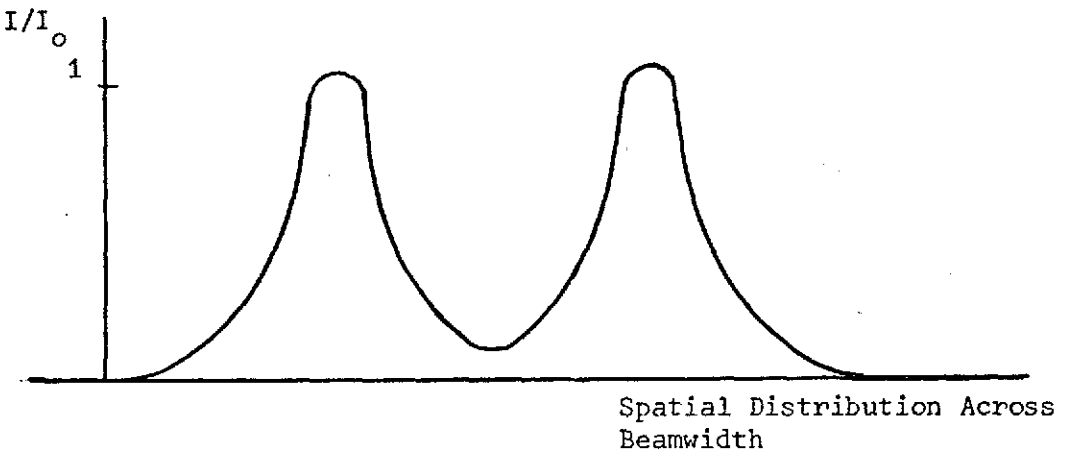

Figure 7. Unrealistic Spatial Distribution of Beam Intensity

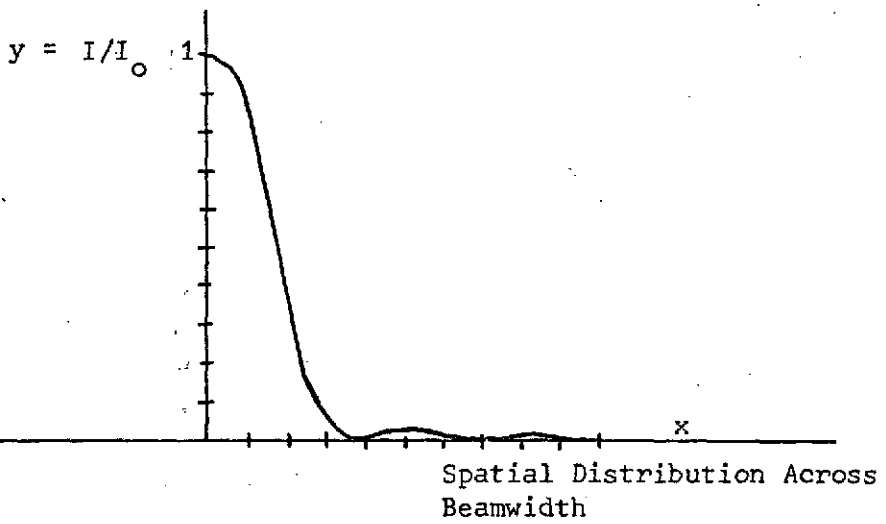

Figure 8. Actual Spatial Distribution of Beam Intensity

2), the intensity is given by: $I(p) = |U(p)|^2$

$$= (2J_1(kaz)/kaz)^2 \, I_o \, ,$$

where I_o = the maximum intensity, $J_1(kaz)$ is the first order Bessel function with the argument kaz where a = the radius of the circular aperture, z = the radius of a particular point in the diffraction pattern, and k = the magnitude of the wave number = 2 pi/λ. The function

$$y = (2J_1(x)/x)^2$$

is plotted in figure 8. Since the second maximum has an intensity of 0.0175 times that at x = 0, the side lobes will not be important in terms of energy transferred. Figure 9 is a photograph of the actual beam shape recorded as the beam swept past the photodetector.

The equation $I(p) = I_o(2J_1(kaz)/kaz)^2$ may be rewritten in terms of the angle α between the origin (center of the circular aperture) and the particular point on the diffraction pattern (figure 10). Hence, $I(p) = I_o \dfrac{(2J_1(2\pi a \sin\alpha/\lambda))^2}{((2\pi a \sin\alpha)/\lambda)^2}$ (reference 6) using the notation of figure 10. The first zero is the point of importance since virtually 100% of the energy lies within the first null-to-null beamwidth. This occurs when $2\pi a \sin(\alpha)/\lambda = 3.8$, or $\sin(\alpha) \doteq \lambda/2a$. However, for α small, $\sin(\alpha) \doteq \alpha \doteq z/L$, hence $z = \lambda L/2a$. We can therefore see that z varies linearly with L and the null-to-null beamwidth, 2z,,also varies linearly with L.

The beam therefore retains its basic shape but diverges to encompass a larger area as the separation between sender and receiver is increased.

The beam divergence is a fixed quanity specified for a given laser. For the 0.75 mw laser used (19 cm mirror separation), the max-

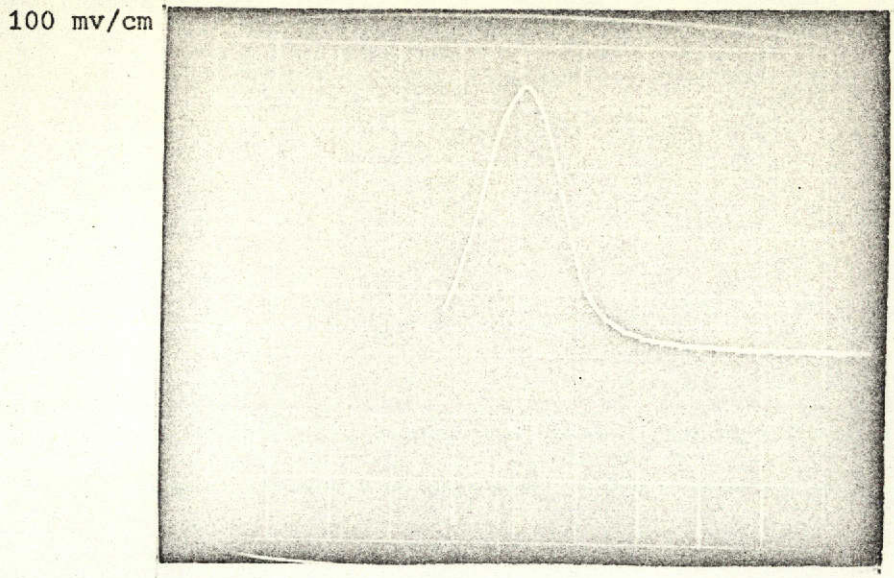

Figure 9. Photograph of the Spatial Distribution of the Laser Beam

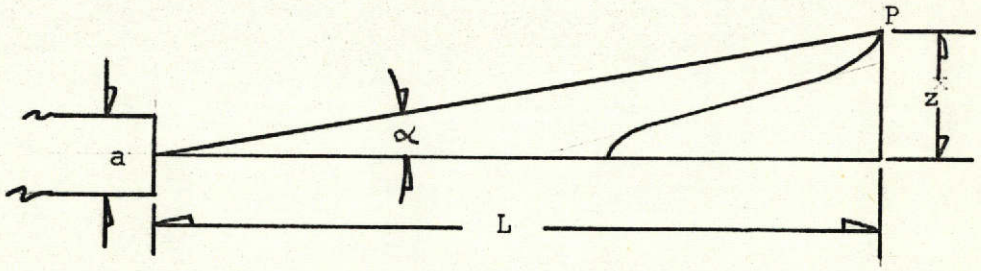

Figure 10. Fraunhofer Diffraction at a Circular Aperture

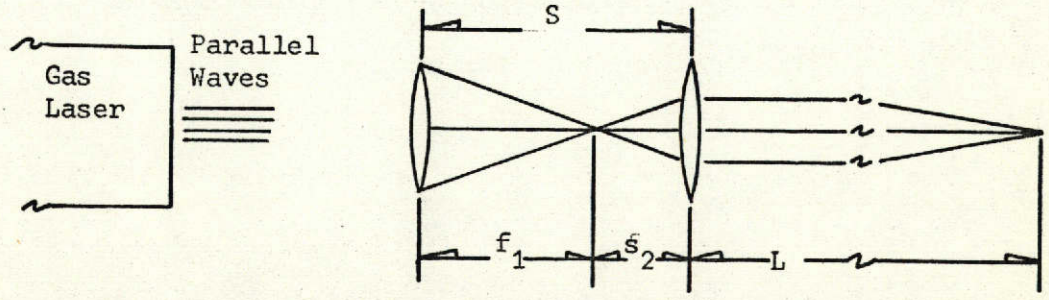

Figure 11. Optical Telescope Used to Limit the Beam Divergence

imum beam divergence is given as 1.5 milliradians. At the aperture the beamwidth is 1.2 mm; we can therefore calculate the beamwidth at any distance by the simple relation $z = L(1.5)(10^{-3})$.

When the distance is 1000', z is 1.5'. When the distance is 100', z is 1.8". The 1.8" beamwidth is quite acceptable at 100', but at 1000' the 1.5' beamwidth implies that the spatial power density (mw/cm^2) is too low and the signal to noise ratio correspondingly low. This naturally leads us into a consideration of limiting the maximum beam divergence to around 3 to 4 inches at 1000'. This is accomplished using an optical telescope focused at 1000' and not at infinity. Figure 11 shows the physical set-up.

Optical Control of Beam Divergence

Assume that the laser source is an effective infinite source;ie, the beam is plane parallel. The Gaussian form of the thin lens equation (reference 3) is $1/s + 1/s' = 1/f$,

where f is the focal length of the thin lens, s is the object distance, and s' is the image distance. We have therefore,

$$1/f_1 = 1/s_1 + 1/s_1' ,$$

where s_1 = infinity. Hence, $1/f_1 = 1/s_1'$.

Also, $1/f_2 = 1/s_2 + 1/s_2'$,

where $s_2' = L = 1000'$. Lens L_1, was chosen with a focal length f_1 = 5cm; lens L_2,with a focal length f_2 = 9 cm. We therefore calculate the separation between the two lens as: f_1 = 5 cm, $s_2 = f_2 s_2'/(s_2' - f_2)$, which implies s_2 is a number slightly greater than f_2. Since $s = f_1 + f_2$, a slide adjustment for the lens was incorporated into the design. (Refer to Plate 1))

Estimation of the Laser Power Necessary at the Instrument's Maximum Range

The amount of incident light on the photodiode which produces a signal equal to the noise generated internally by the photodiode is called the noise equivalent power (NEP) (reference 1). This is the minimum detectable signal level. There are two mechanisms for noise production, shot noise in the photodiode and thermal resistor noise in the external circuit. Following UDT's Design Manual,

$$V_s = (2eI_oB)^{\frac{1}{2}} R_L ,$$

where V_s is the shot noise, e is the electronic charge, I_o is the dark current, B is the bandwidth, and R_L is the load resistor. Also,

$$V_T = (4kTBR_L)^{\frac{1}{2}} ,$$

where V_T is the thermal noise voltage generated in R_L. And,

$$V_1 = i_1 R_L ,$$

where V_1 is the light generated signal voltage in R_L. It is seen that i_1 consists of two parts, a steady DC part due to sunlight bias, and the pulsed part due to the swept laser beam.

The signal to noise ratio is

$$S/N = i_1 R_L / ((4kTBR_L)^{\frac{1}{2}} + (2eI_oB)^{\frac{1}{2}} R_L)$$
$$= i_1 / ((2eI_oB)^{\frac{1}{2}} + (4kTB/R_L)^{\frac{1}{2}}).$$

The NEP occurs when SNR = 1, hence when

$$i_1 = ((2eI_oB)^{\frac{1}{2}} + (4kTB/R_L)^{\frac{1}{2}})$$

or

$$NEP = R_L((2eI_oB)^{\frac{1}{2}} + (4kTB/R_L)^{\frac{1}{2}})$$
$$= i_1 R_L ;$$

where R_L = 100K ohms, I_o = 0.5 uamps (PIN-10 at 10 volts backbiased), T = 300°K, k = 1.38×10^{-23} J/°K, e = 1.6×10^{-19} coulombs, and B = 1 Hz (see reference 1). Hence, NEP $\doteq$ 8×10^{-7} watts/Hz$^{\frac{1}{2}}$. The problem now remains to determine the power available at 1000' with the given sweep

rate with the 0.75 mw laser. The time it takes a circular pulse to cross the 0.5" detector junction at 1000' is given approximately by $t = x/rw$, where $v = x/t = rw$, x being the beamwidth at 1000' (around 3"), $r = L = 1000' = 12{,}000"$, and $w = 2\ pi\ f = 2\ pi$ radians. Therefore, $t \doteq 40$ useconds, the crossing time. The bandwidth is therefore roughly given by $B = 1/t = 25$ KHz. Hence, the power per $Hz^{\frac{1}{2}}$ is 0.75 mw/25KHz = 4.8×10^{-6} watts/$Hz^{\frac{1}{2}}$. We can therefore see that the 0.75 mw laser being swept at 1 Hz will theoretically have enough power to send a detectable signal out to the upper limit of 1000'.

Physical Mount and Alignment Proceedure

In order to be able to align the beam scanner with the photodiodes, the laser, servomotor, and optics were mounted on a transit (plate 2). The beam was carefully adjusted to be parallel to the optical sight of the transit telescope wuch that a target mounted on the receiver serves as an alignment method. Also, as in similiar measuring proce=dures, the photodetector mount bar should be situated to be perpendicular to the optical sighting direction and should be leveled. Methods, procedures, and associated errors due to the positioning of the bar can be found in any standard Civil Engineering handbook.

There exists a problem in alignment which could cause measurement errors. If the plane of rotation of the beam does not coincide with the plane formed by the photodiodes, there will be a discrepancy between the real distance and that measured. The diagram below indicates this.

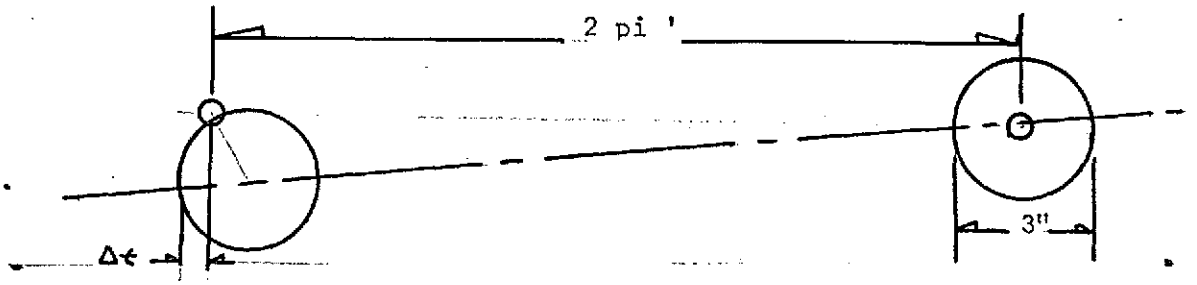

The worst case would be at 1000' when the spot diameter is around 4". The error in the measurement is due to the Δt, where the maximum deviation $\Delta t \doteq 8$ msec at 1000'. Hence the error would be 8 usec/1 msec = .8%. It is therefore imperative that the beam sweep be in the same plane as the photodiodes.

Electronics for Information Processing

The final item to be considered is the electronic data processing. Two pulses are received from the two photodetectors. These pulses are to a first approximation consinusoidal and of rather small amplitude. This is observed in figure 9. The time interval between these two pulses varies inversly with the distance. The system must accurately measure this separation and then invert it to obtain the distance measured. An averaging process should be incorporated into the system to reduce the effect of random errors. Lastly, the separation is to be displayed directly in feet in order to minimize measuring time and to avoid time consuming--error producing steps. See plate 4. Chapter 2 now considers in detail the system electronics.

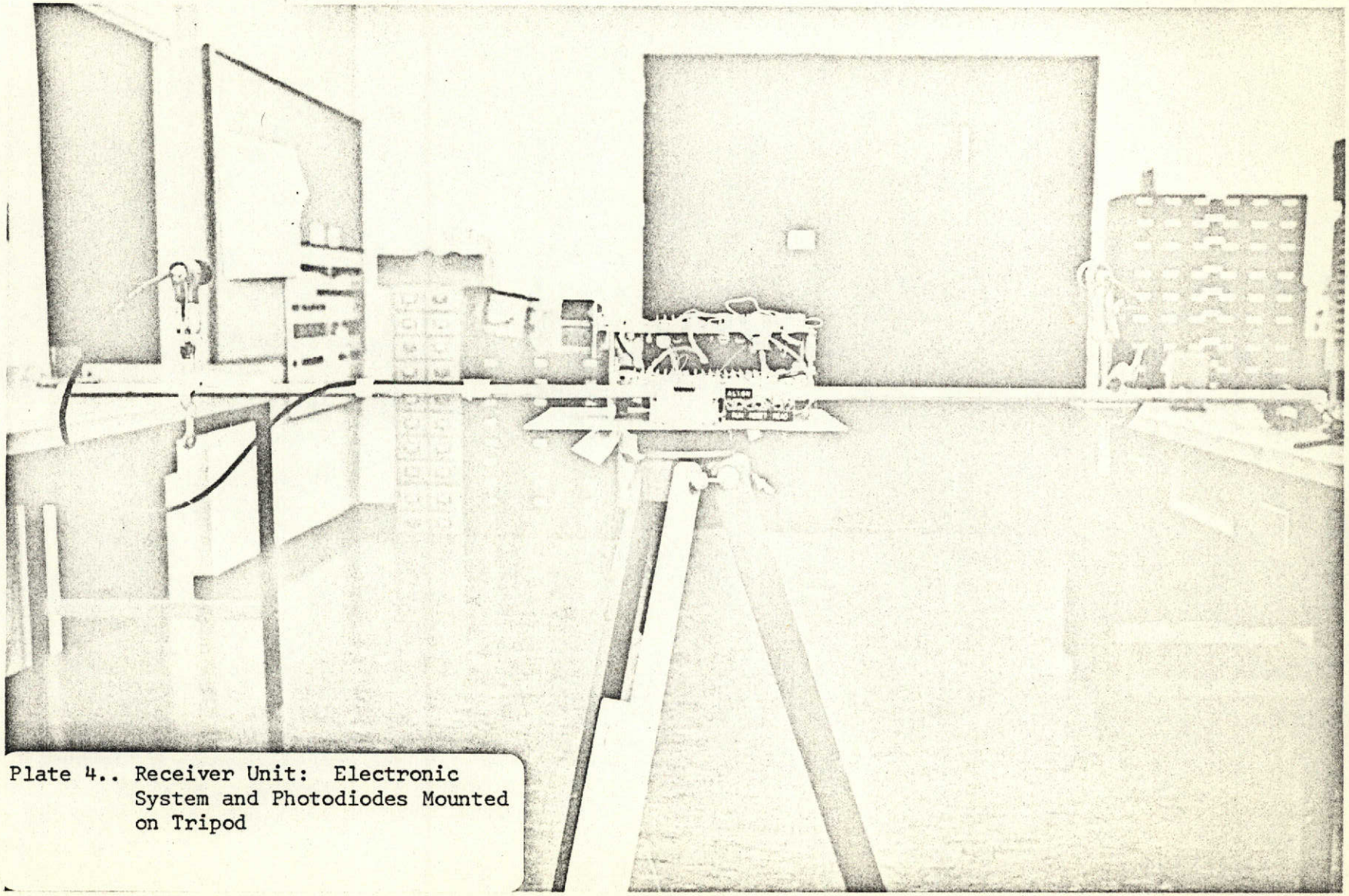

Plate 4.. Receiver Unit: Electronic System and Photodiodes Mounted on Tripod

CHAPTER III

CIRCUIT DESIGN

The purpose of the information processing section is to convert the data received by the photodetectors to a numerical readout of the distance between the transmitter and receiver. Figure 12 blocks out this section.

Photodiode, Amplifier, Filter, and Comparator

Blocks #1 and #2 consist of the pulse reception and shaping network. The complete diagram is drawn in figure 13. Note that the photodiode #1 and block #1 is identical to photodiode #2 and block #2.

The optical filter limits the amount of light intensity received by the photodiode to that of light centered on wavelength 6328 angstroms $\pm$ 30 angstroms. The current amplifier is of a standard configuration which reverse biases the photodiode by 15 volts. The reverse bias is desired both to operate in the linear region and to reduce the diode capacitance so as to decrease the risetime.[1] For the PIN-10 diode, the junction capacitance is around 10 pf with 15 volts back-biased. The 100 pf capacitor in the feedback configuration reduces the amplification of the semiconductor shot noise. Figure 14 presents the various circuit waveforms.

The filter section offers bandpass amplification. To study the effect of this network, consider the system in the s-domain:

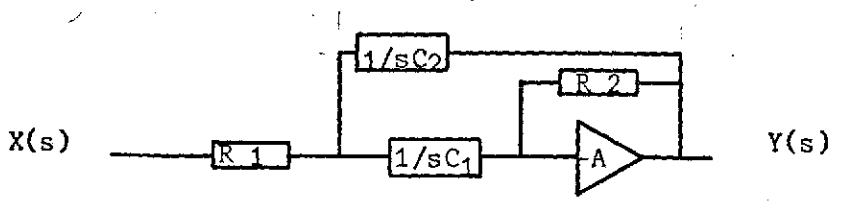

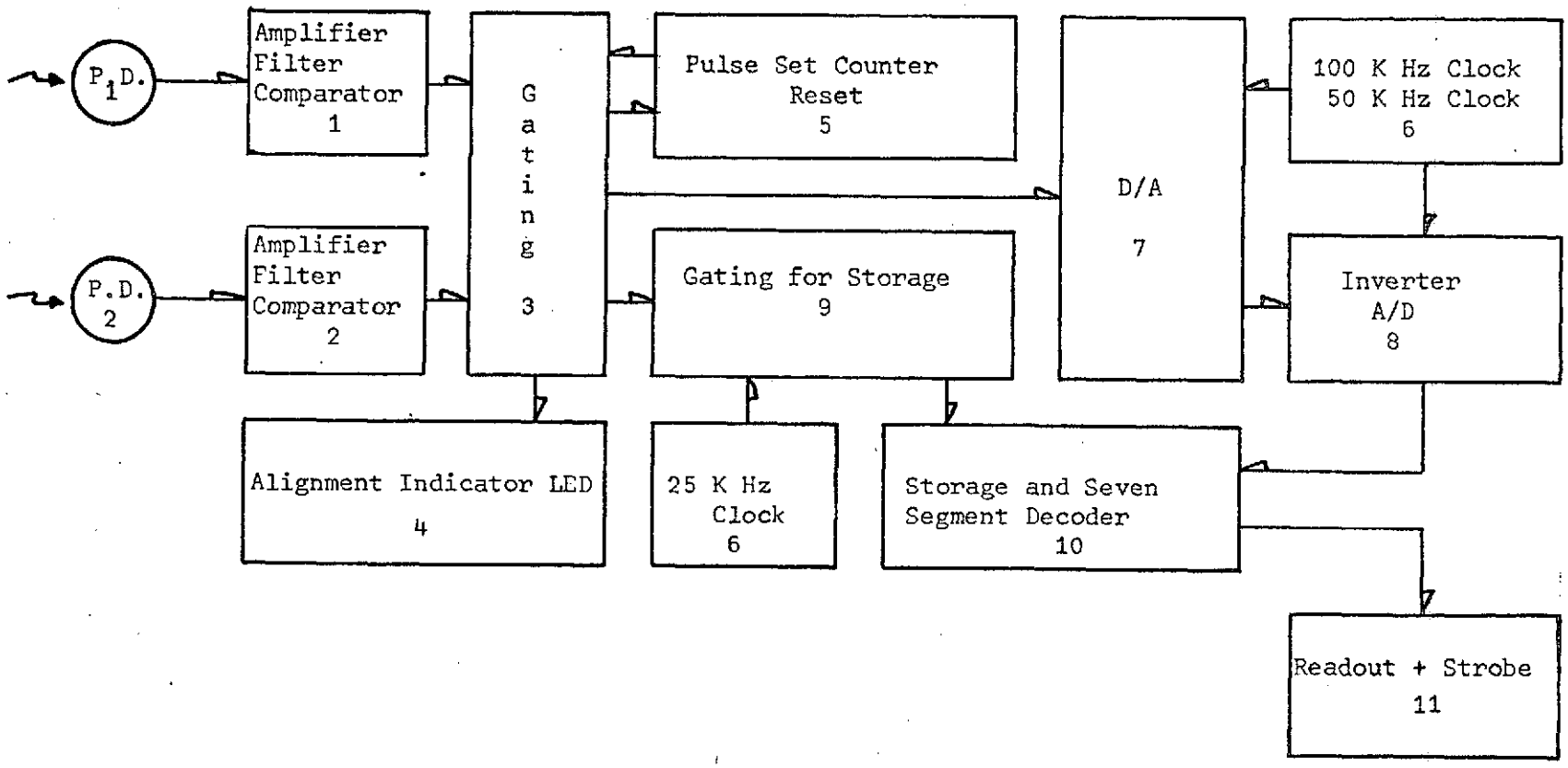

Figure 12. Block Diagram of the System Electronics

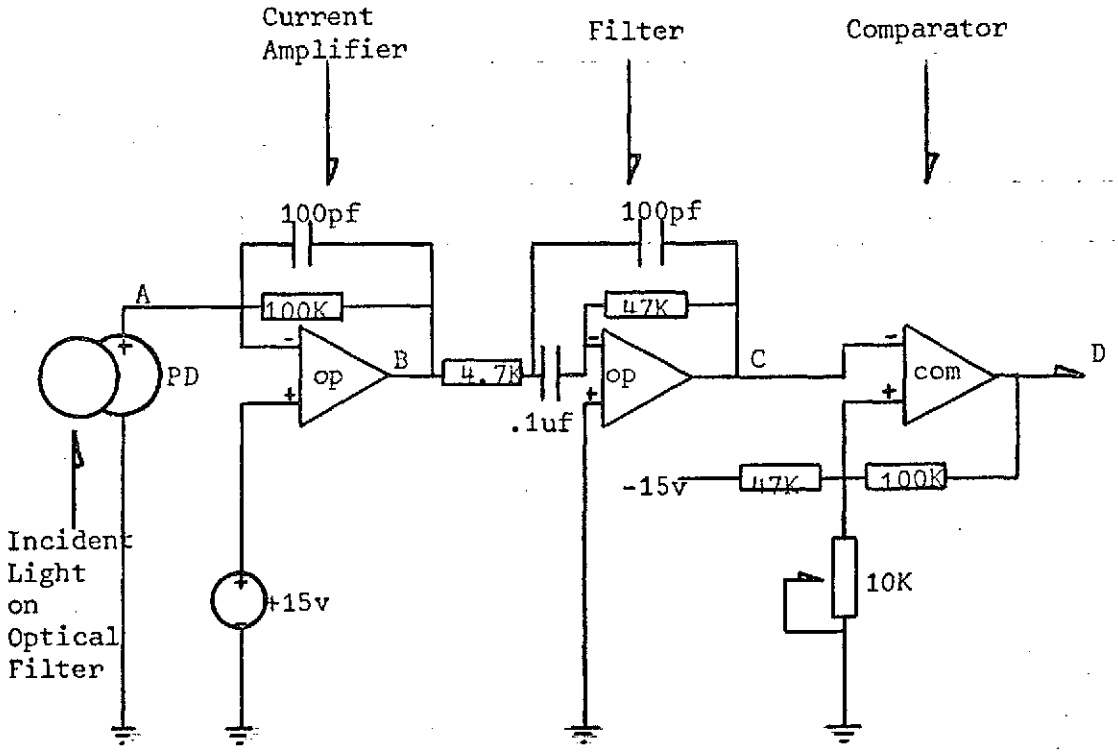

Figure 13. Circuit Diagram for the Receiving Unit: Photodiode, Amplifier, Filter and, Comparator

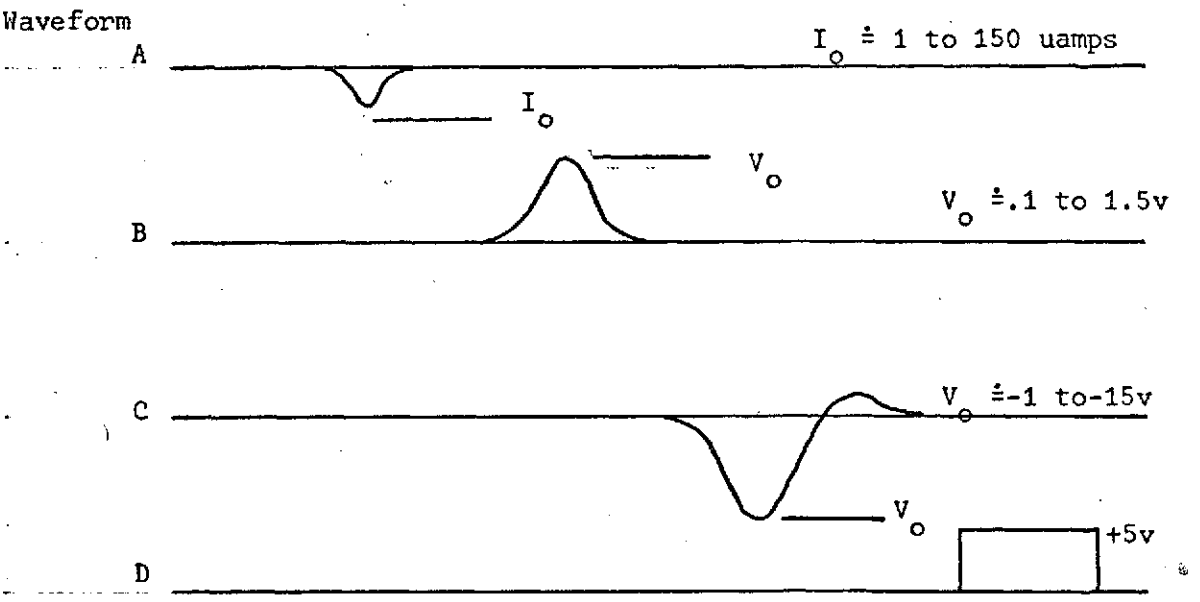

Figure 14. Waveforms for Block #1 and #2

Standard analysis gives us the system transfer function

$$H(s) = (-R_2/sC_2)/(R_1/sC_2 + R_1/sC_1 + R_1R_2).$$

The s can be replaced by jw and the magnitude of the transfer function described by $H(jw) = aw/(b^2w^2 + (1 - w^2c)^2)^{\frac{1}{2}}$,

where $a = R_2C_1$, $b = R_1(C_1 + C_2)$, and $c = R_1R_2C_1C_2$. This function of w, the angular frequency, was numerically evaluated and plotted as a function of the frequency, f. The results are computer plotted in figure 15. From the graph, we see the 3 db lower cutoff point at around 400 Hz, the upper at around 39 K Hz, and the maximum centered at 3 K HZ. The reason a bandpass was selected over a high or low pass was, at the low end, to eliminate any low frequency changes in the DC bias signal by, of example, relatively slow changes in cloud formation; and, at the high end to reject shot noises in the detectors. The primary requirement of the filter is that it pass all of the possible signal frequencies.

To investigate the nature of the frequency spectrum of the signal, consider the input signal pulse in the time domain at the two extreme ranges as depicted in figure 16, where T has been calculated using 2T = x/rw = Beamwidth/L(2 pi)(f). At a distance of 100', T_{100} = 66 usec., and T_{1000} = 20 usec. We can approximate the function $(J_1(x)/x)^2$ by a cosine function within the first null-to-null range. Hence, the function to be transformed into the frequency domain is the much simplified f(t) = cos(pi t/2T), for /t/ $\leq$ T. Therefore, taking the Fourier Transform results in

$$F(jw) = \int_{-\infty}^{\infty} f(t)\exp(-jwt)dt = \int_{-T}^{T} \cos(\pi t/2T)\exp(-jwt)dt$$

$$= \int_{-T}^{T} \cos(\pi t/2T)\cos(wt)dt$$

$$= T\,\frac{\sin(\pi/2 - wt)}{(\pi/2 - wt)} + T\,\frac{\sin(\pi/2 + wt)}{(\pi/2 + wt)}.$$

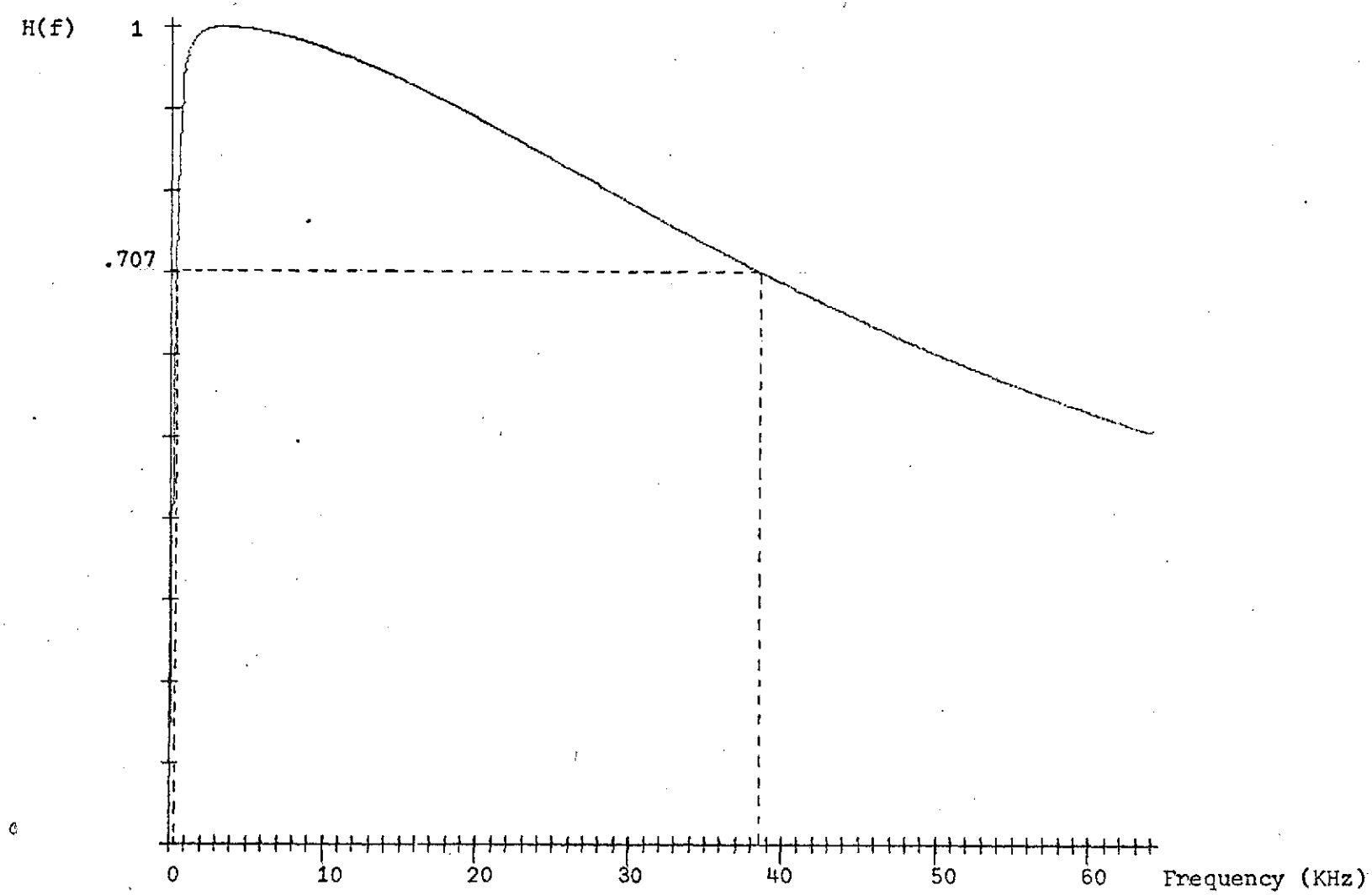

Figure 15. Magnitude of the Transfer Function Plotted as a Function of Frequency

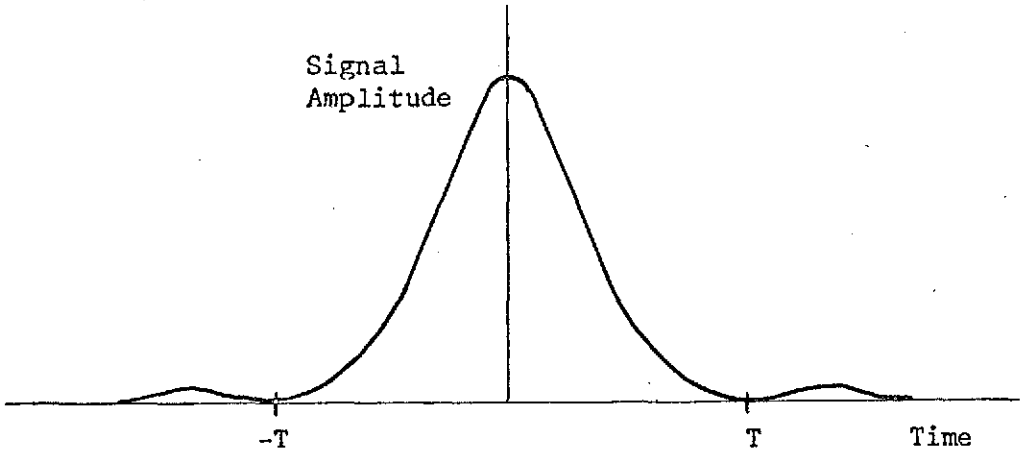

Figure 16. Input Pulse Signal in the Time Domain

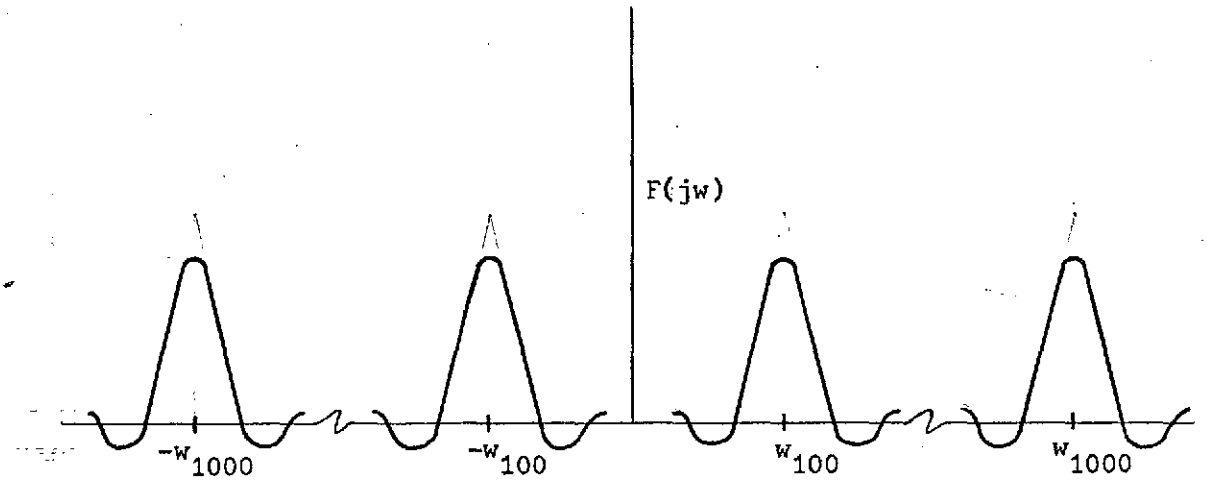

Figure 17. Fourier transform of Input Signals

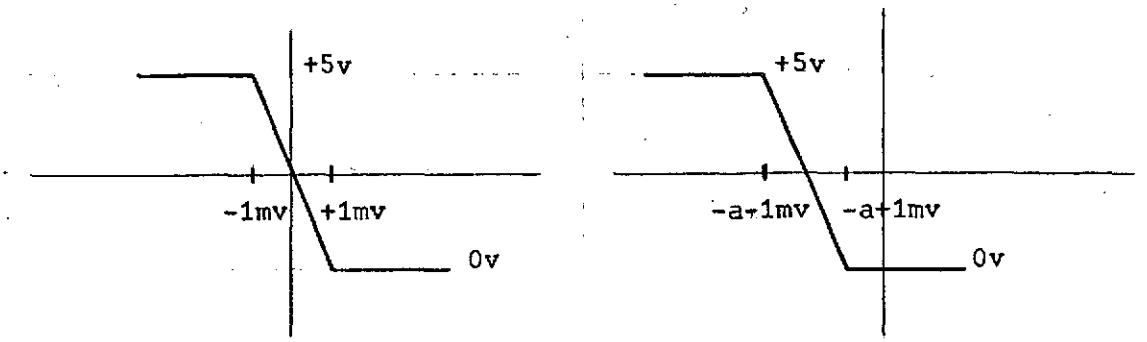

Figure 18. (a) Comparator Function with Zero Threshold (b) With Negative Threshold

The second term in the expansion of exp(-jwt) drops out because the integral of cos(pi t/2T)sin(wt) over symmetrical limits is zero. Figure 17 sketches these functions. The major peak occurs where w = pi/2T. At 100', 2 pi f_{100} = pi/2T_{100}, or the frequency is given by f_{100} = 1/4T_{100}. At 1000', f_{1000} = 1/4T_{1000}. Since T_{100} = 66 usec, and T_{1000} = 20 usec., we have that f_{100} = 3.8 KHz, and f_{1000} = 12.5 KHz. The first null of interest occurs where pi/2 + wT = -pi or where 3 pi/2 = wT. At 100', $f_{100null}$ = $3f_{100}$. Therefore the minimum value occurs where $f_{100\ min}$ = $f_{100}/3$ = 1.3 K Hz. The maximum occurs where $f_{1000\ null}$ = $f_{1000\ max}$ = $3f_{1000}$ = 37.5 K Hz. Therefore, the upper and lower cutoff points should be around 40 K Hz and 1 K Hz, respectively.

The value of R_1,R_2,C_1, and C_2 were therefore selected as R_1 = 4.7 Kohms, R_2 = 47 Kohms, C_1 = 0.1 uf, and C_2 = 100 pf, which gave the lower cutoff as $f_L \doteq$ 400 Hz, and the upper cutoff as $f_U \doteq$ 39 K Hz. The general waveshape at point C after the filter is shown in figure 14.

The last element in this section is the comparator. Its function is two-fold; first, to establish a threshold trigger voltage, and second, to change any analog voltage to a digital 5 volts--0 volts logic level. See figure 14. Figure 18 exhibits its characteristics for (a) zero threshold level (+ input grounded) and (b) -1.5 volts threshold level used in the actual design.

The constant may be varied from 0 to -2.5 volts. It's value is set just above the threshold of noise which may vary depending upon the atmospheric conditions--bright sunlight as opposed to an after sunset measurement.

Gating

Block #3 in figure 19 represents the section of the circuit which

prepares the pulses to be used in such a manner so as to extract the desired information. The circuit is depicted in figure 19.

The pulses as appearing at D are positive going--inverters I_1 and I_2 switch the polarity of these pulses and AND GATE 1 adds these inverted pulses which gives the results at E as:

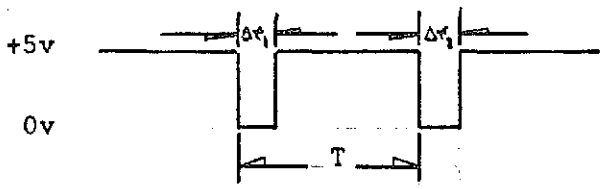

where T is the quanity of interest. The reason for manipulation of the pulses into this form is to be able to use the leading edge of the input pulses from the photodiode to perform the logic functions to follow. If the trailing edge were used, then the possible different reactions of blocks 1 and 2 to varied signal intensities expecially to saturation (which may occur at the lower ranges) would result in a time error $e = |\Delta t_1 - \Delta t_2|$, not readily predictable. Thus by using the leading edge, times Δt_1 and Δt_2 become irrelevant.

The AND GATE 2 guides the pulse set into block #5 which counts 40 pulse sets (40 pairs of pulses) and then disables the upper input to AND GATE 2.

The JK flip-flop 1 has its Q output high for the duration of the pulses, time T. Hence, at Q_1 the following pulse is present

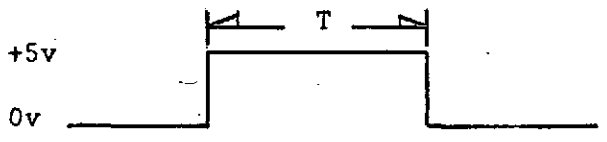

The positive pulse is then sent to the D/A (digital to analog) converter which converts the time information (pulse length T) into a negative analog voltage. The JK flip-flop FF2 has its Q output Q_2, go high at the

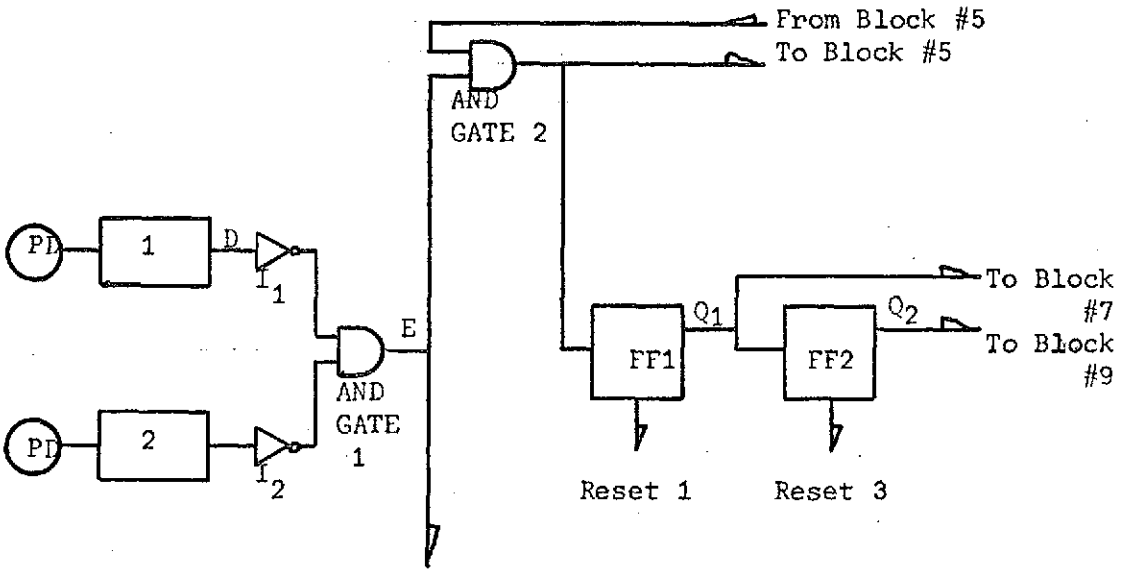

Figure 19. Block #3: Gating Circuitry

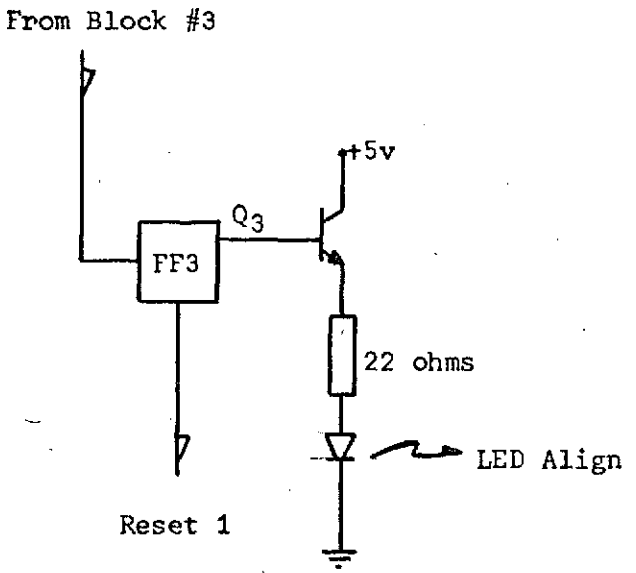

Figure 20. Block #4: Alignment Circuit

termination of the pulse at Q_1.

Alignment LED

Block #4 consists of a flip-flop whose Q output indicates, by means of a transistor and LED (light emitting diode), a correct pulse sequence. The LED is on during the time between the two leading edges of the output of AND GATE 2. If the sweep beam is blocked during the 1 msec to 10 msec interval when it passes across the photodetectors in such a manner that only one photodiode receives a pulse, then the LED will indicate that the reading is erroneous and must be repeated by remaining almost constantly on except for the 1 to 10 msec. The circuit for Block #4 is drawn in figure 20.

Pulse Set Counter and Reset Function

Block #5 counts 40 pulse sets and then disables the entire measurement process. This offers an averaging process for 40 separate measurements. Forty pulse sets were chosen as a compromise between time of measurement and accuracy. The block essentially consists of 4 flip-flops in a divide by 10 mode. It also contains a light emitting diode which lights-up after the measurement to indicate that the process is terminated. Lastly, it has the manual reset which resets the complete system preparing it to make another measurement. The Circuit is shown in figure 21.

Let the period of the input pulses be given by the diagram at the top of page 29. Since the total period between subsequent pulse sets is 1 second, the time remaining between the end of the pulse of width T, and the remaining part is given by: $1 - T = a$. The period of the pulse sequence at Q_4 is $T + a$ (figure 22). Therefore, the period of FF 5 output Q_5 is $2(T + a)$; of FF 6, Q_6, is $4(T + a)$; of FF 7, Q_7, is $8(T + a)$;

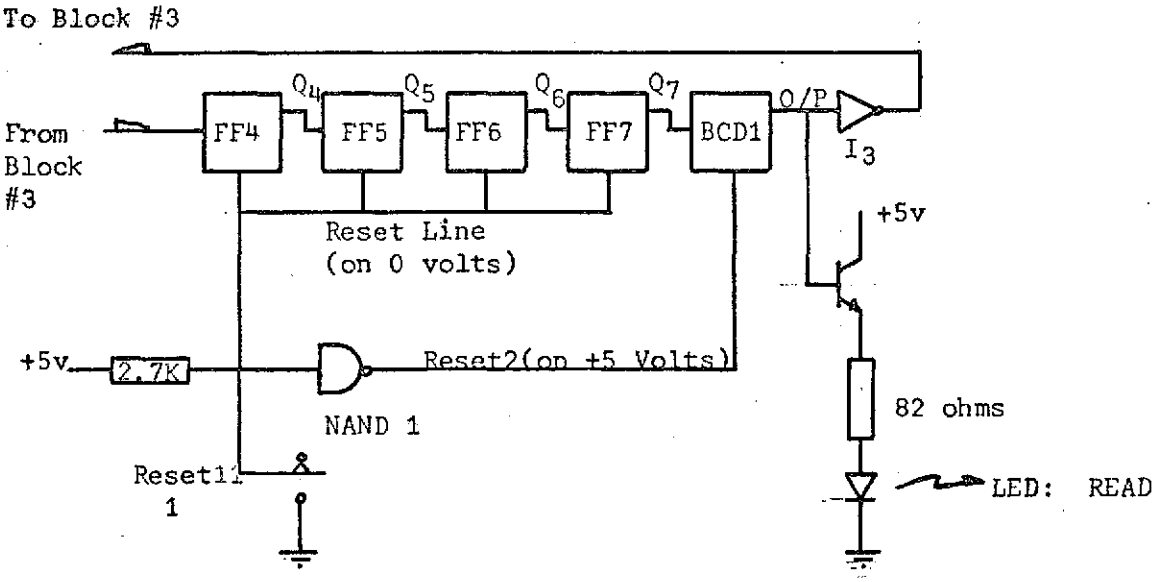

Figure 21. Block #5: Pulse Set Counter and Reset Function

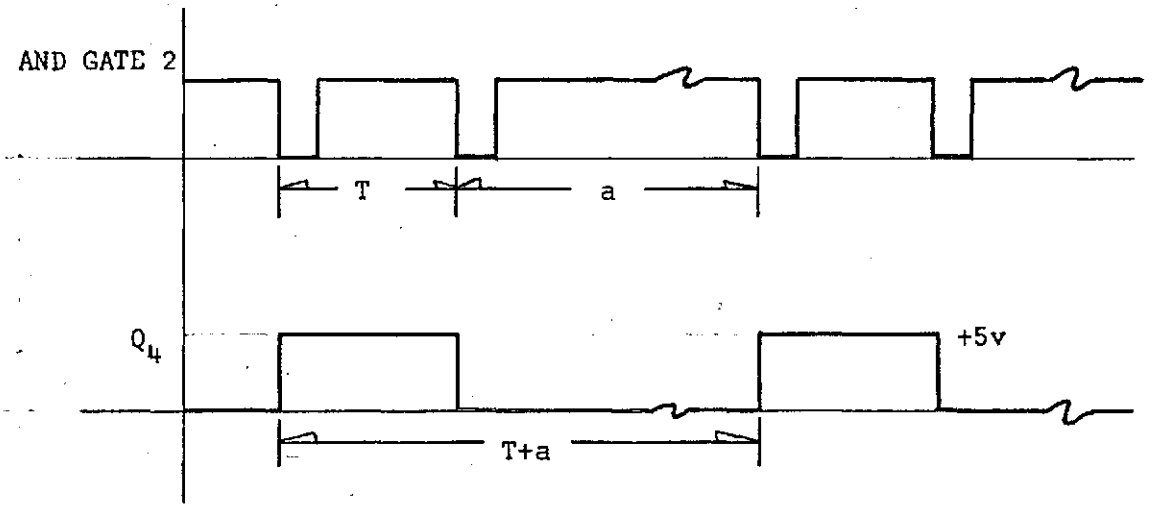

Figure 22. Waveforms for Block #5

and, finally the output of the divide by 10 is 80(T + a). Since the counting sequence stops when the output of BCD 1 (binary-coded decimal) goes high, the period is halved: 40(T +a). Since T + a = 1 second, after 40 seconds the measuring process is terminated.

Clock

Since the transition from a pulse of width T to an analog voltage occurs by means of a process of counting clock pulses, it is imperative that the clock be extremely precise and stable. This immediately implies a crystal oscillator. There are three basic clock rates of interest: 100 KHz, 50 KHz, and 25 Hz. These are derived from the basic 100 KHz clock oscillator by divider circuits. See figure 23.

Digital to Analog Converter

The information pulse Q_1 of width T is gated with the 100 KHz clock and fed into a series of 3 BCD counters. The outputs of these three counters is fed into a digital to analog converter which converts the 12 BCD inputs into a negative analog voltage. Note figure 24. This conversion step is necessary in order to be able to invert the number proportional to the pulse width by the "Hybrid-Optiverter"--an analog to digital converter. The two inputs to the AND GATE 3 are inherently asynchronous; ie, there is no possible way to synchronize the onset of the pulse from Q_1 with the clock.

During the time when Q_1 is high, the 3 counters count pulses from the 100KHz clock. At the close range (100'), Q_1 is high for 10 msec. (T = 10 msec.). This allows (10msec)(100 KHz) = 1000 pulses to be counted. This corresponds to a -10 volt output from the D/A. At the far end (1000'), Q_1 is high for 1 msec. (T = 1 msec.). This allows (1 msec)(100 KHz) = 100 pulses to be counted up. This corresponds to a

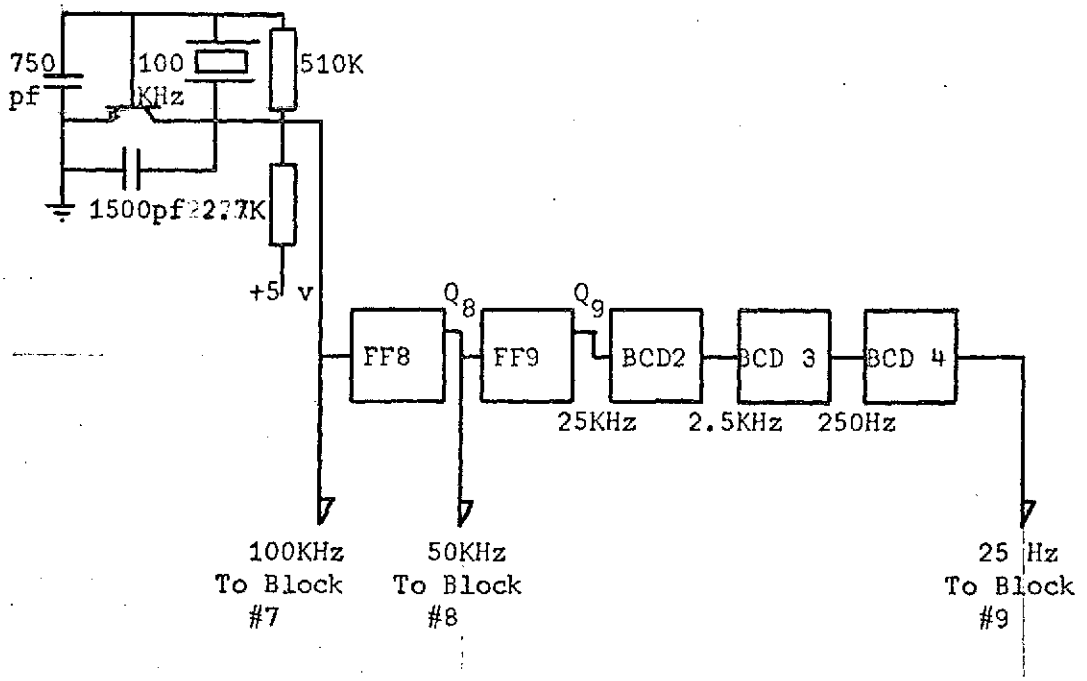

Figure 23. Block #6: Crystal Clock and Divider Circuit

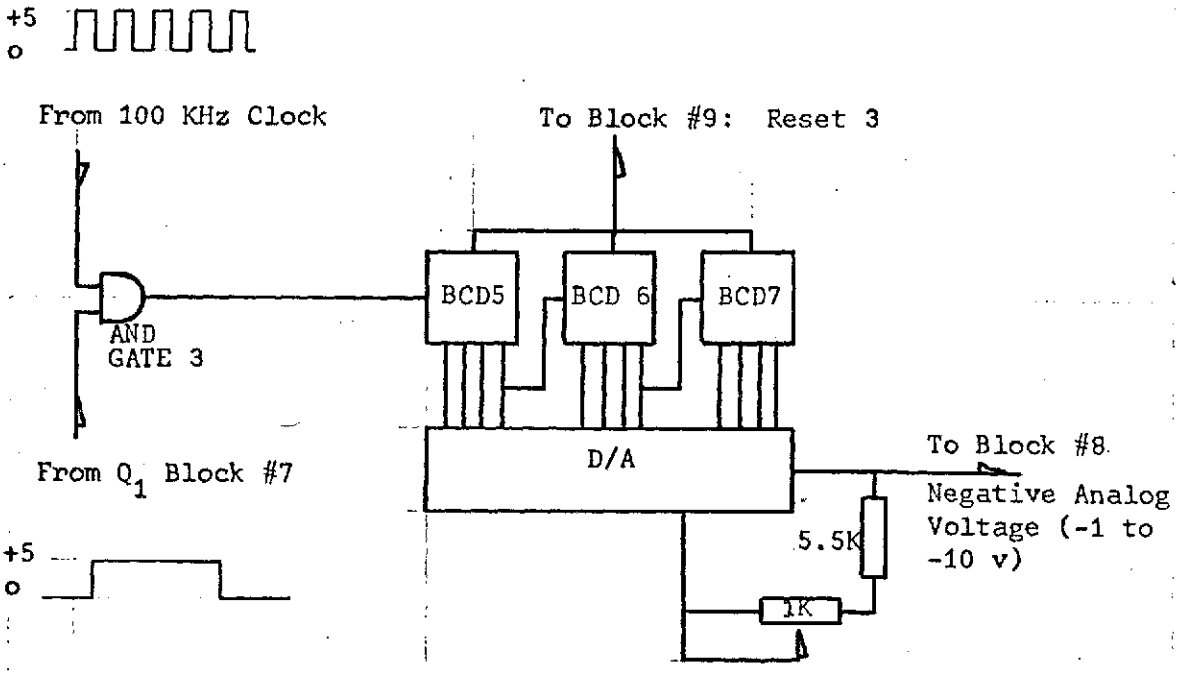

Figure 24. Block #7: Digital to Analog Converter

-1 volt output from the D/A.

Inverter and A/D Converter

The purpose of the so-called Hybrid-Optiverter chip is to convert the analog voltage to a pulse density proportional to the inverse of the analog input. The dual-in-line chip consists of an op-amp, comparator, and flip-flop (see figure 25). These in conjunction with a FET transistor in the feedback loop accomplish the inverting function.

The function of the optiverter is as follows: The positive constant current source feeds into a summing junction (point A in figure 25) of the op-amp; also, a variable negative current from the D/A feeds into the same junction. The 0.03uf capacitor serves as an integrator and when the FET is pinched off, it charges with a constant slope due to the constant source. When the constant input current causes the comparator to change states the FET is turned on for one clock period (50 KHz). Th This allows the capacitor to gain a positive charge (with respect to the inverting input of the op-amp) which is proportional to the magnitude of the input from the D/A. With a large positive charge on the capacitor, a relatively long time will be necessary to bring the junction of the op-amp to cross the zero voltage level to cause the comparator to switch states which causes the flip-flop to change states on the subsequent clock downstroke. Since the output is taken as the $\overline{Q}$ of the flip-flop, a large negative voltage implies a low pulse density--likewise, for a small negative voltage, a large pulse density will be obtained because the charge on the capacitor never departs far from the zero voltage axis. At all the in-between voltages, there is a direct linear relationship.

There is now available a pulse density which is proportional to

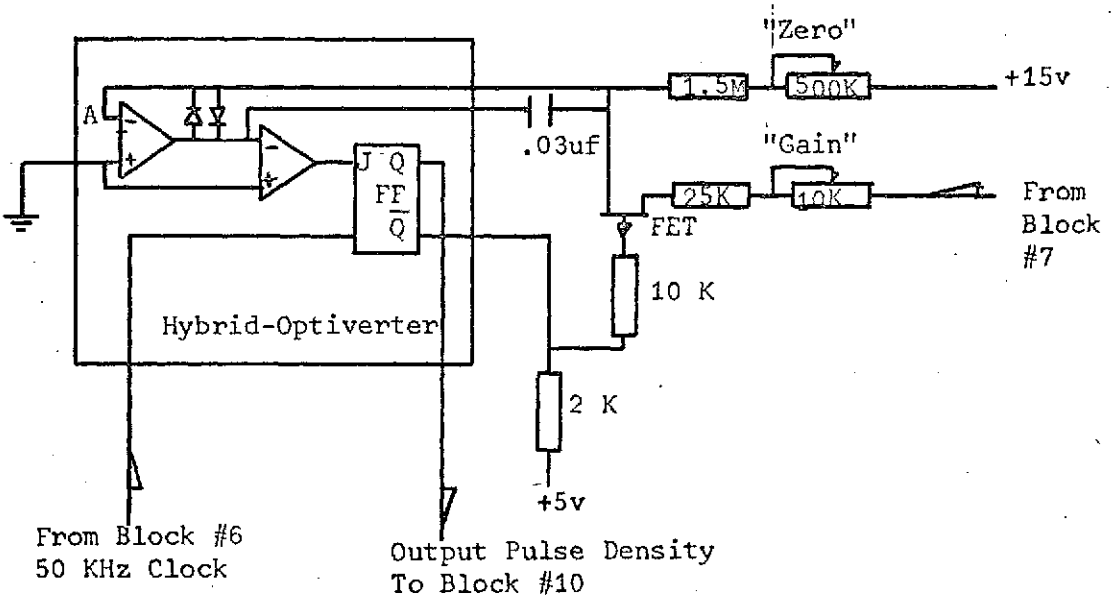

Figure 25. Block #8: Inverter and A/D Converter

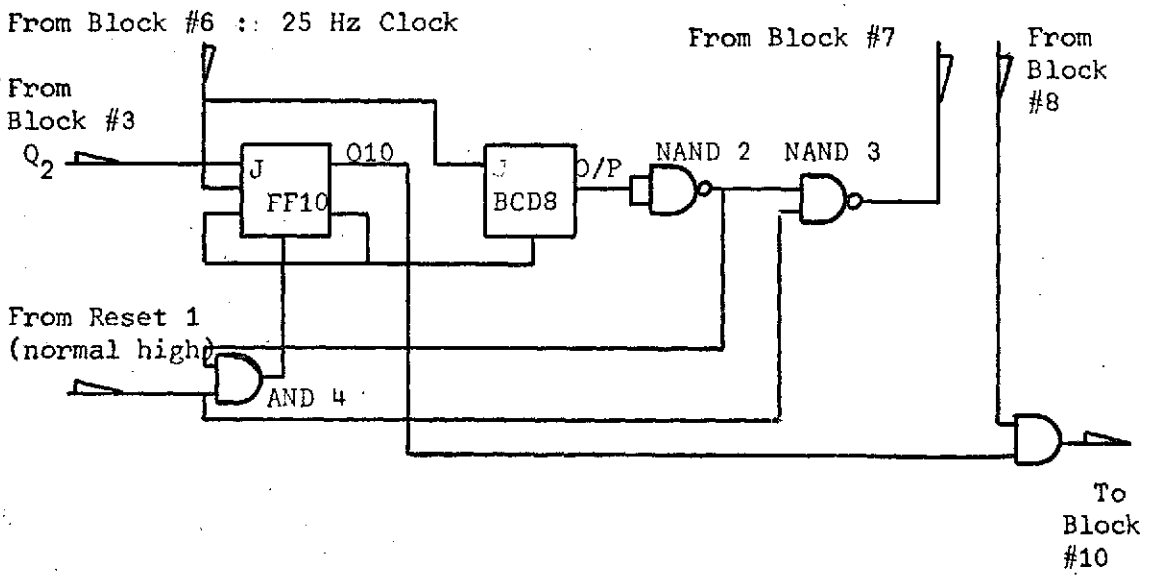

Figure 26. Block #9: Gating for Storage

the inverse of the magnitude of the D/A voltage. However, since the D/A voltage is directly proportional to the time interval, the pulse density is inversely proportional to the time interval, T. The constant of proportionality is obtained by adjusting the potentiometers controlling the inputs to the Hybrid-Optiverter. This is also the process of calibration. One establishes an accurate base line and then adjusts either the D/A or the A/D to give the specific distance readout.

Gating for Storage

At the output of the optiverter there is a pulse density proportional to the distance between the transmitter and receiver. Block #9 (figure 26) is the logic which samples this pulse density for 200 msec and allows this sample to be stored additively on a series of counters. The timing diagram for this process is displayed in figure 27.

The timing diagram is rather self-explanatory indicating that Q_{10} is the gating pulse which allows the pulse density from the Hybrid-Optiverter to be applied to the counter of block #10 for 200 msec at which time the NAND gates reset the FF 10,FF 2, and subsequently the BCD 8. It should be noted that the 200 msec is very stable--the stability being due to its derivation from the crystal clock.

Storage and BCD Seven Segment Decoder

Block #10 receives the 200 msec sample 40 times. Each sample is added to the previous one. It's diagram is presented in figure 28. At the end of the 40 pulse sets there is stored a number on the five counters. In block #11 there is a strobing unit which sends positive logic pulses to the NAND gate thru OE1 to OE5 in a uniform sequence at a rate of 500 Hz. The reason for this is because it is desired to use a single LED chip for the numeric readout. With only 14 pins access-

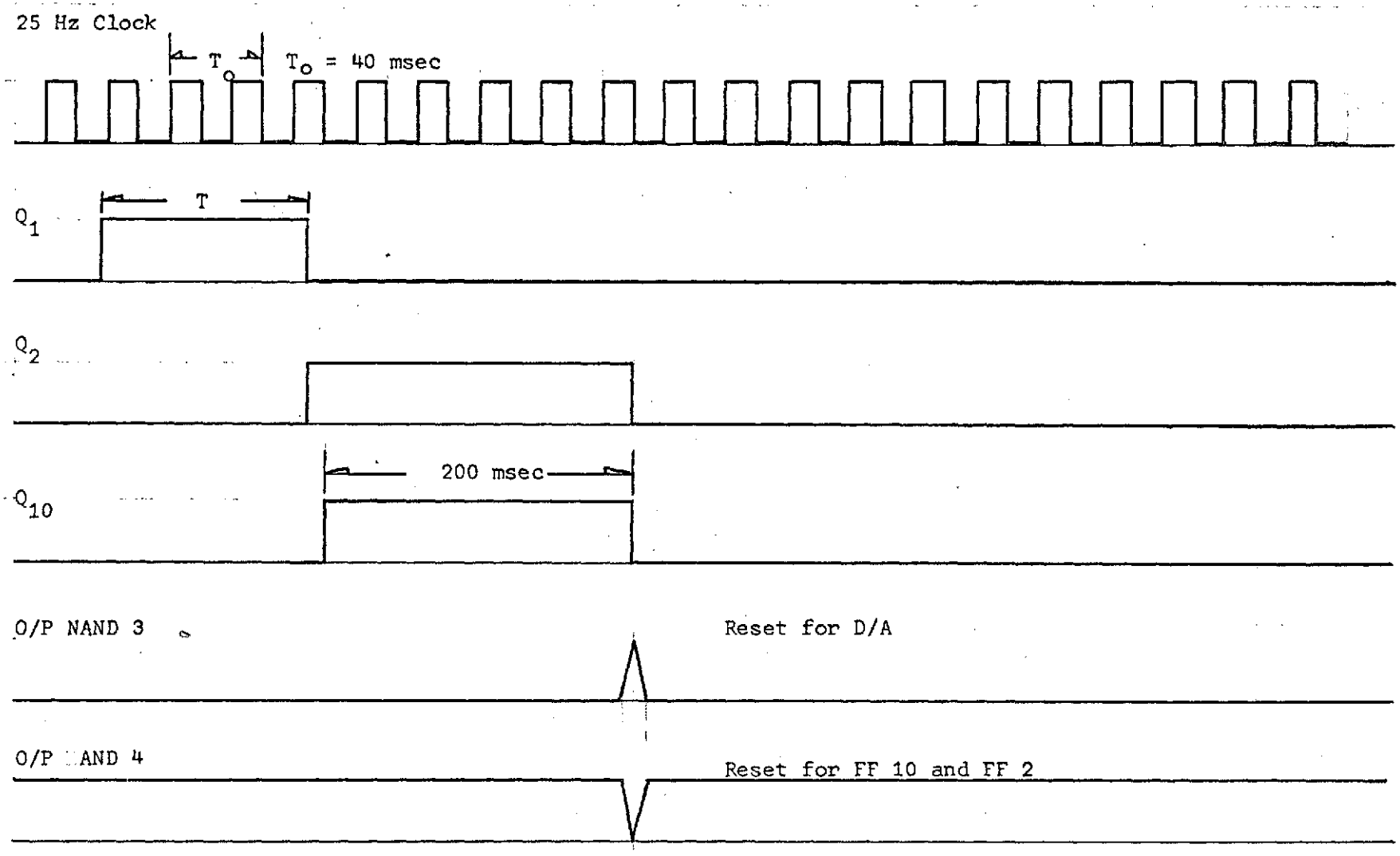

Figure 27. Timing Diagram for Block #9

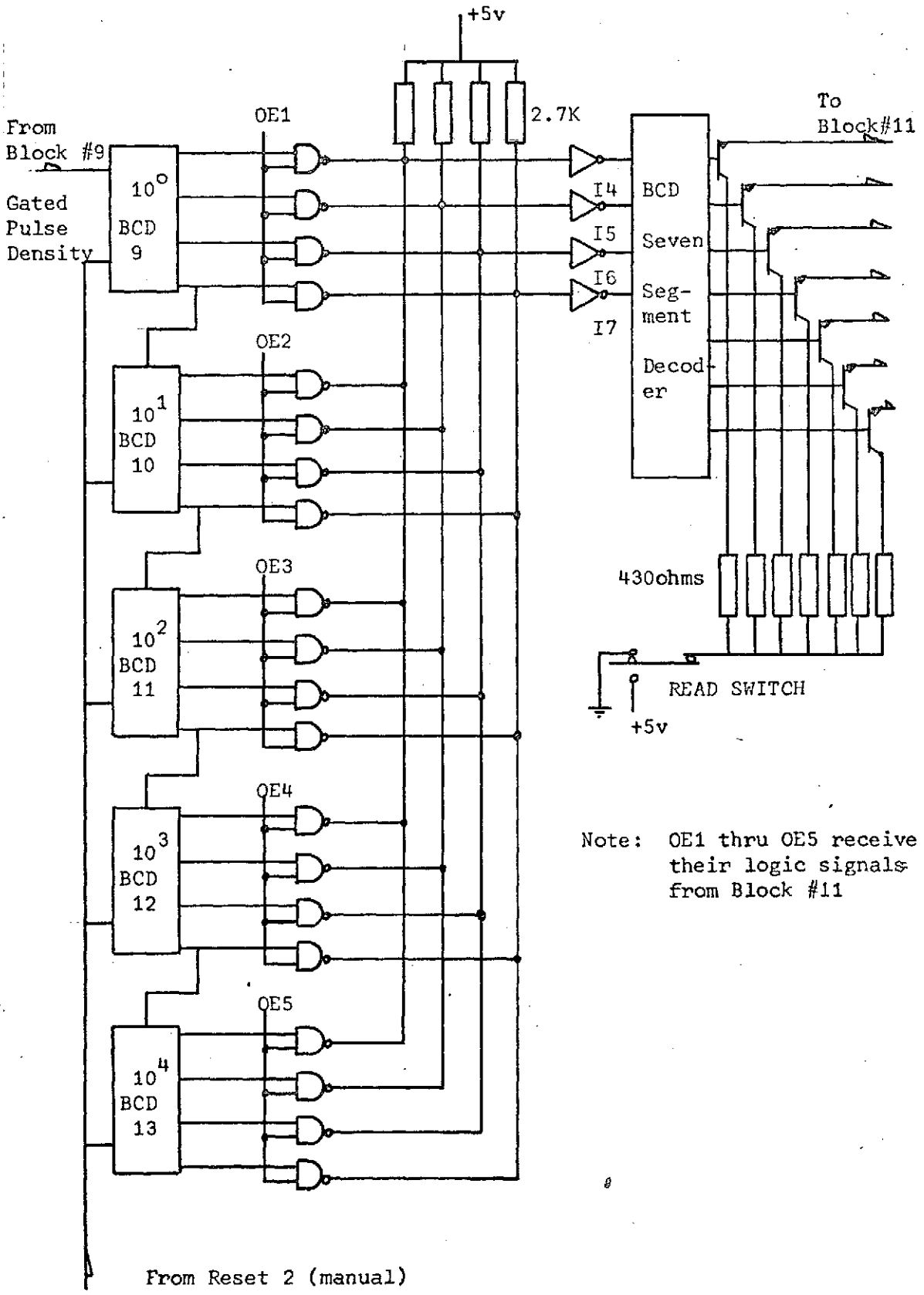

Figure 28. Block #10: Storage and BCD Seven Segment Decoder

ible for 5 digits, the unit must be strobed in order to obtain the five digits appearing constantly displayed. The BCD to Seven Segment Decoder converts the BCD logic into the seven segment code necessary for the readout which has seven segments per digit.

Readout and Strobe

The readout displays at command whatever information is stored in the 5 counters by actuating the switch in figure 28. This switch enables the various LED's in the chip to be energized. The readout chip and strobe are drawn in figure 29.

The hysteresis controlled NAND gate is an astable multivibrator which causes the BCD to count up and when applied to the TTL 1/10 decoder a pulse sequence is established which progressively causes OE1 thru OE 5 to go high at a rate determined by the astable multivibrator, in this case 500 Hz.

As can be seen when, for example, OE3 is high, the information from the third BCD counter is transferred to the seven segment decoder and the third digit is enabled so that the information stored is displayed.

In order to obtain a sense of unity, a timing diagram for the entire circuit is included in figure 30.

There are a sum total of 40 pulses sets accepted, after which time input signals are not processed; ie, BCD 1 remains high. FF 1 (Q_1) gates the clock for each pulse set period, T. The output of the D/A produces a negative analog voltage proportional to the number of counts accepted. The optiverter generates a pulse density inversely proportional to the negative analog voltage, which is gated into the storing counters for 200 msec. Each separate reading is obtained by reseting

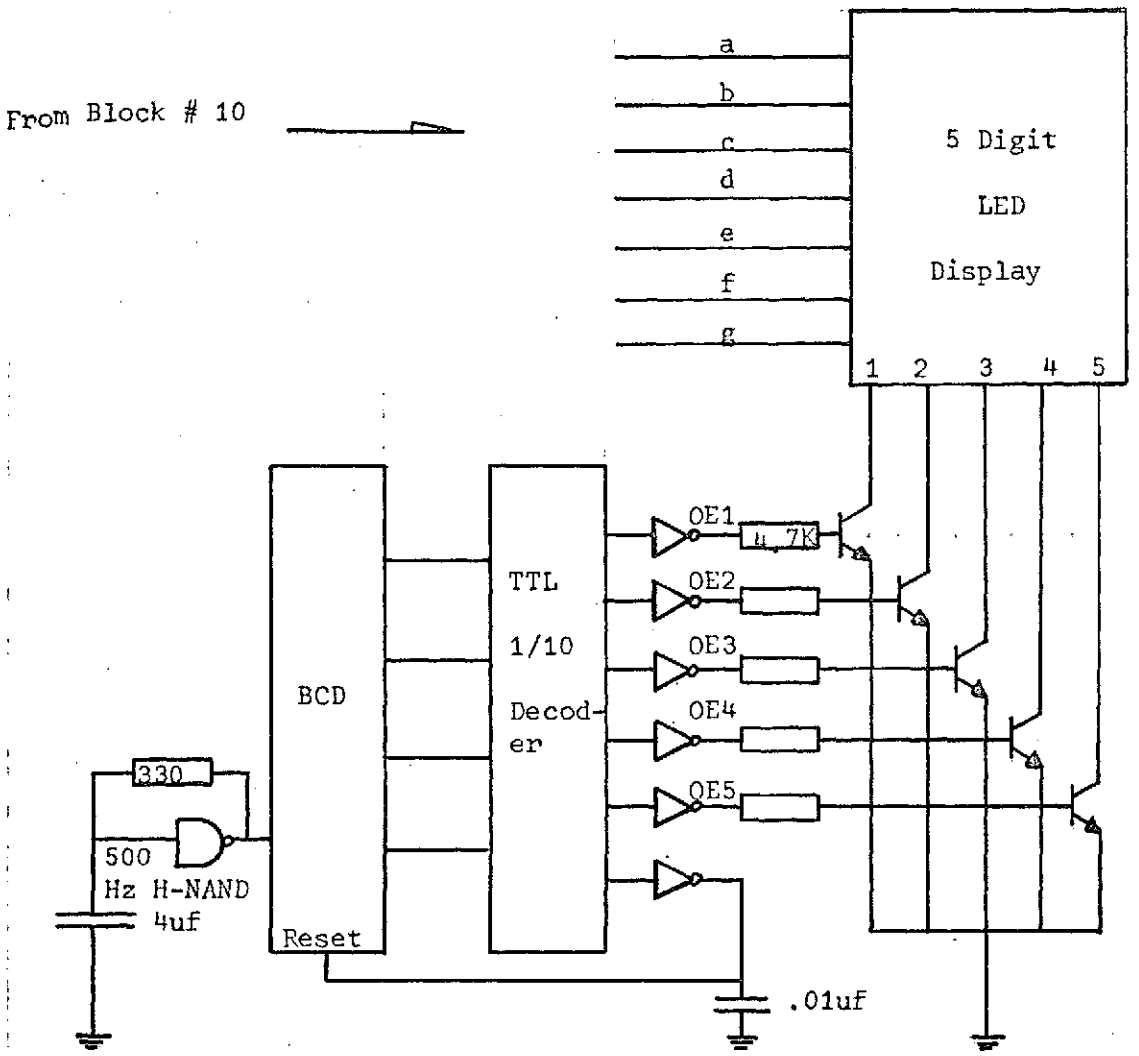

Figure 29. Block #11: Readout and Strobe

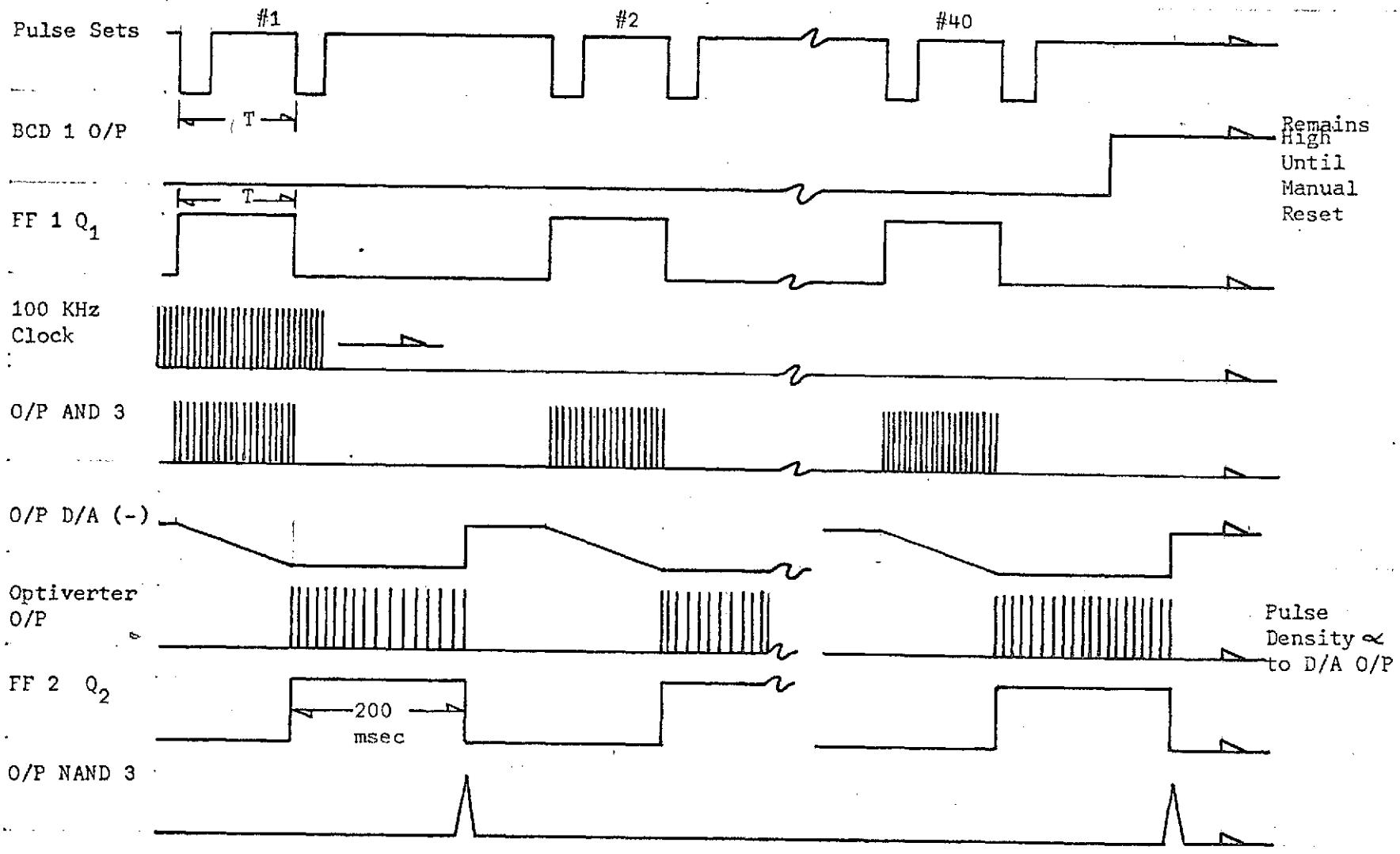

Figure 30. Timing Diagram for the Complete Circuit

all but the pulse set counter after each pulse set measurement is recorded.

Figure 31 presents the complete circuit diagram.

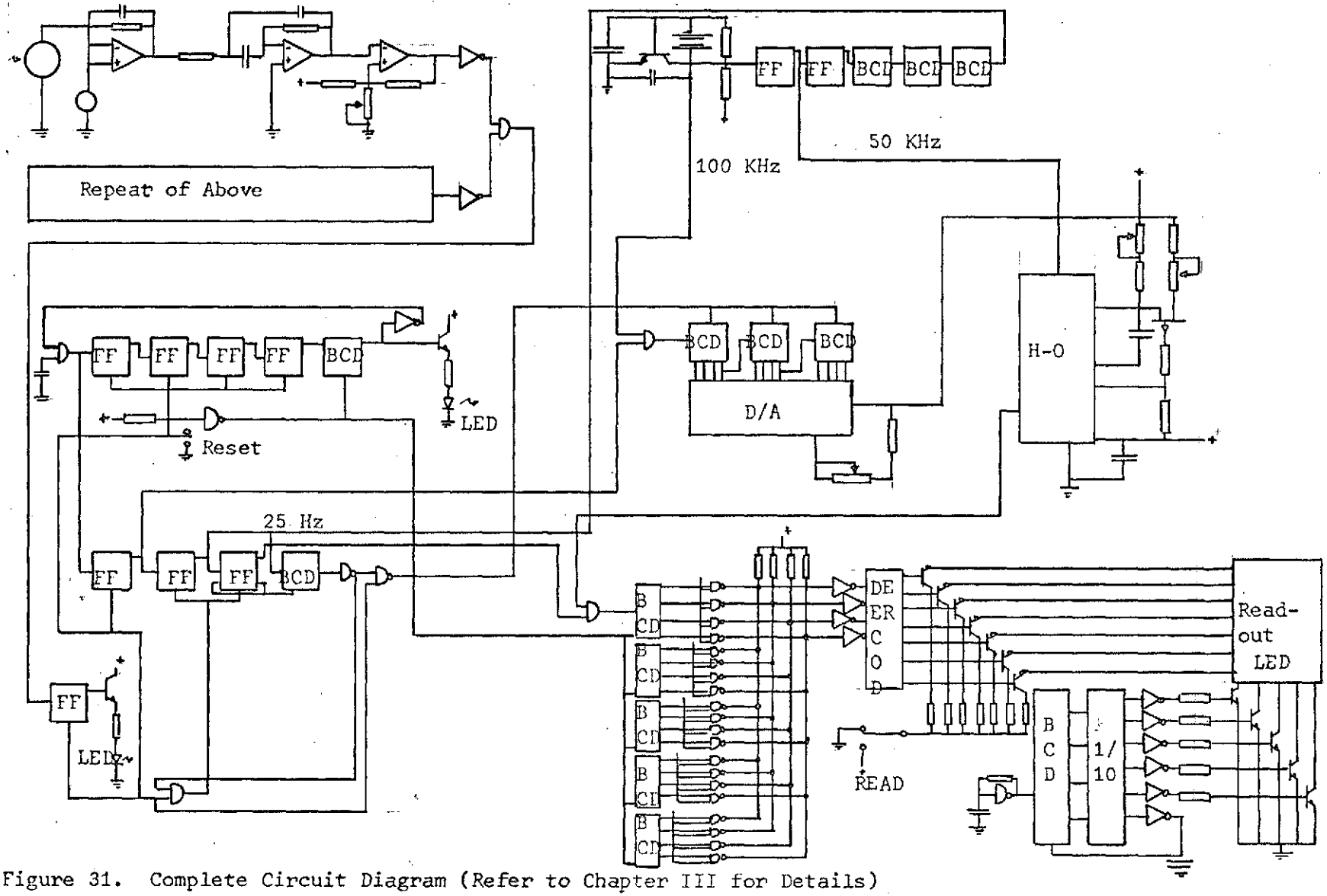

Figure 31. Complete Circuit Diagram (Refer to Chapter III for Details)

CHAPTER IV

RESULTS AND EVALUATION

Whenever a measurement is taken there exists some doubt as to its accuracy. If a series of measurements are taken one observes that each individual reading hovers about some "mean" value. The degree to which the readings arerrepeatable is a measure of the accuracy of the device.

In this distance measuring device there are two essential sources of error: the sweep system and the electronic system. The sweep system consisting of the servomotor will in itself exhibit two types of error--a shift in absolute frequency due to component aging and/or thermal drift, and that due to random temporary incremental frequency variation.

The second source of error resides in the electronic system. In essence, the fact that the information pulse, T, is asynchronous with the clock pulse causes the error. At 100', the counters associated with the D/A receive 1000 pulses. Now, depending on the exact width of the pulse T, there may be a zero or up to 50% probability that the number of pulses accepted will vary by one pulse. This is realized from the diagram in figure 32. Notice that when there is exactly an integral number of periods T, then the probability that a pulse will be added or subtracted is one half. Under the worst conditions where $P = \frac{1}{2}$ at 100', there is a variation of 1 pulse per 1000 pulses or 0.1%; at 1000', there is a variation of 1 pulse per 100 or 1%.

Of the two sources of error, it is inferred that in the present system the electronics is the major source of error. Long term (times greater than 40 seconds) shifts in absolute frequency of the servomotor is not a factor because the frequency is adjustable and can be set to the

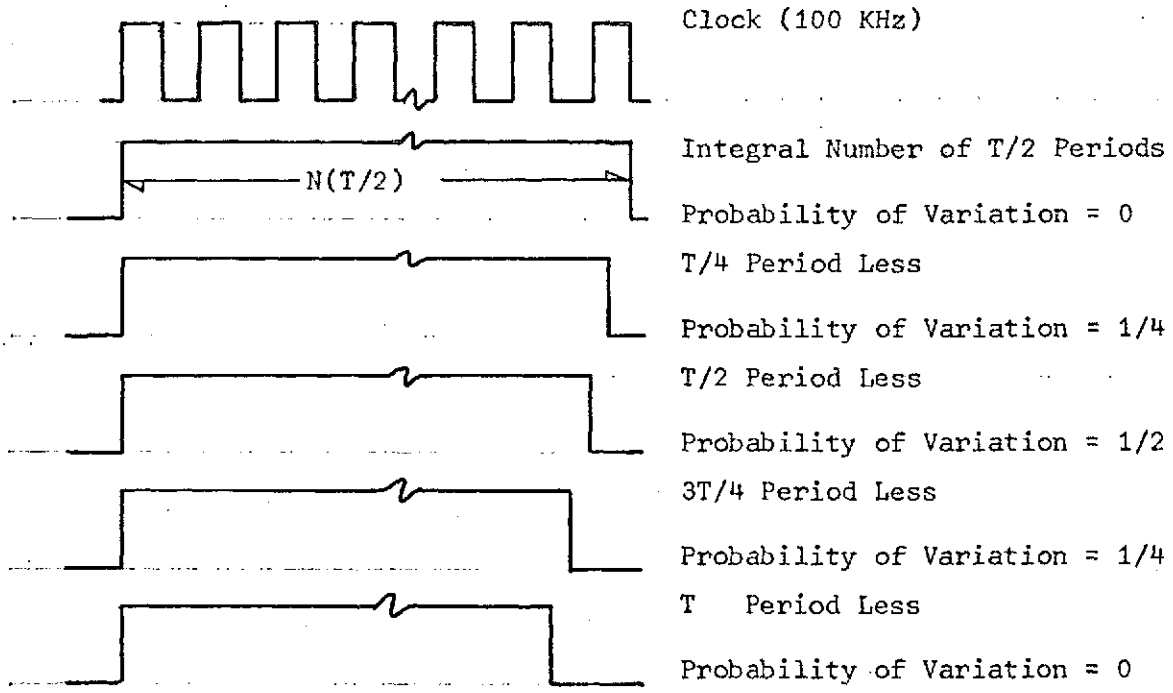

Figure 32. Probability of a Pulse Variation

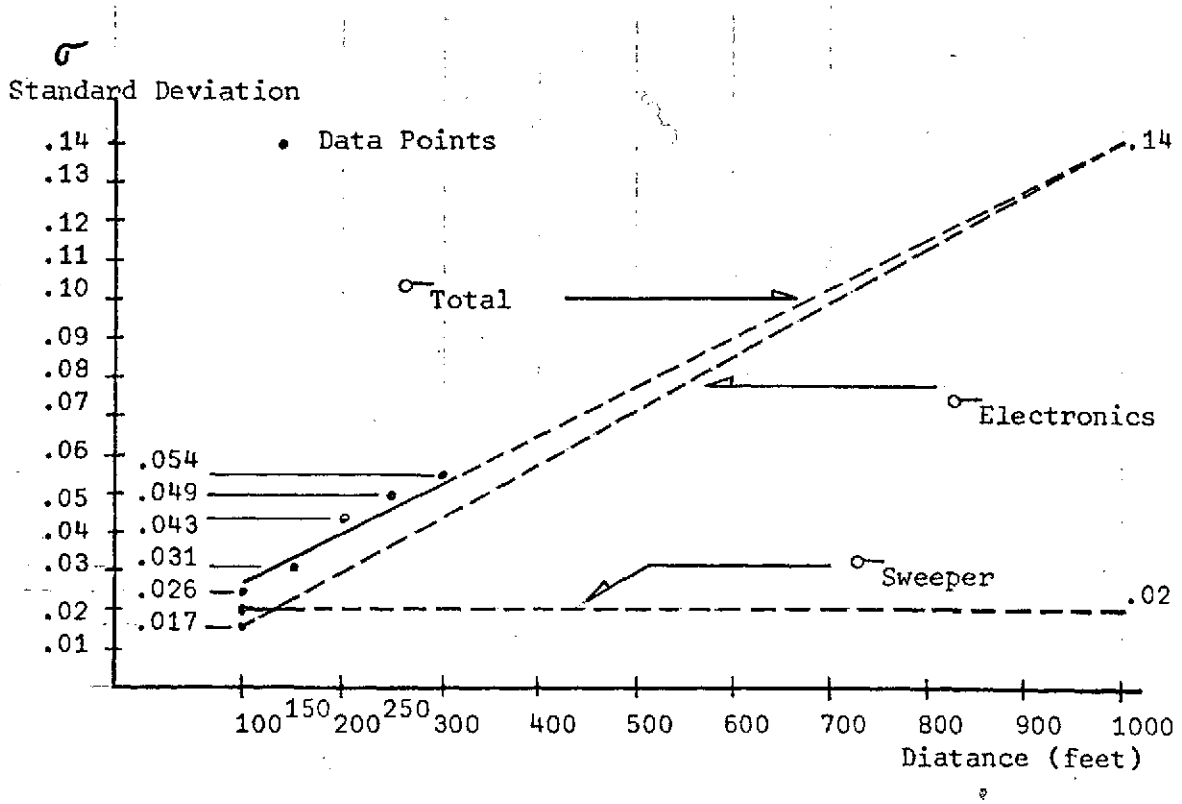

Figure 33. Standard Deviation of the Instrument Over Its Projected Range

desired frequency. However, random shifts are still present and cannot be completely averaged out in 40 pulse set readings. The magnitude of the random error from the electronics alone was recorded at 100' and is seen to comprise approximately one half of the standard deviation squared of the readings. We now infer that because the effective measuring time varies between 10 msec and 1 msec out of 1000 msec (1% maximum) that the nature of the random error will not vary over the entire measuring range. Hence it is concluded that σ_s (standard deviation of the sweeper) is constant over the complete range (figure 33).

Tables I and II present the data recorded from 100' to 300' as actually measured by the instrument. Also included is data recorded by the electronics using two pulse generators instead of the beam sweeper. This was done in order to obtain the standard deviation of the electronics alone. Unfortunately, the pulse generators were not sufficiently stable in order to obtain accurate information about the standard deviation at the longer distances (small pulse separation).

The standard deviation as calculated by the equation given on page 6 where n = 30 is plotted as a function of distance up to 300' and extrapolated to 1000' assuming linearity presides (figure 33). Also drawn are the standard deviations of the sweeper and electronics.

If the assumption is made that the two sources of error are independent, the standard deviation squared of the total unit can be separated as $\sigma^2 = \sigma_S^2 + \sigma_E^2$, where the S and E stand for sweep and electronics respectively. Also assuming that the standard deviation due to the sweeper remains constant, the two curves can be separated and depicted as in figure 34.

Since the standard deviation for second order measurements should

TABLE I

DATA RECORDED BY INSTRUMENT

Distance	100'	150'	200'	250'	300'
Reading					
1.	100.12	150.23	200.11	250.07	300.09
2.	.16	.14	.08	.17	.19
3.	.09	.23	.03	.07	.08
4.	.18	.19	.10	.13	.05
5.	.11	.17	.03	.15	.18
6.	.14	.14	.05	.05	.03
7.	.16	.20	199.98	.02	299.98
8.	.14	.15	.02	.07	.10
9.	.14	.13	.14	.14	.05
10.	.12	.17	.10	.08	.02
11.	.16	.22	.02	.06	.11
12.	.18	.18	.09	.08	.08
13.	.11	.14	.04	.06	.08
14.	.16	.18	.04	249.99	.11
15.	.16	.20	.04	.05	299.97
16.	.14	.17	.09	.15	.13
17.	.11	.23	.03	.10	.12
18.	.13	.22	.01	.06	.08
19.	.14	.13	.04	249.98	.03
20.	.16	.17	.10	.08	.04
21.	.10	.16	.13	.10	.06
22.	.14	.15	.03	.04	.04
23.	.10	.20	.06	.06	.11
24.	.13	.17	199.99	.10	.00
25.	.14	.20	.01	.11	.10
26.	.13	.19	199.98	.03	.09
27.	.09	.24	.02	.03	299.99
28.	.18	.17	.10	.10	.14
29.	.12	.22	.08	.04	.04
30.	.13	.19	.01	.01	.08

TABLE II

DATA RECORDED WITH PULSE GENERATORS

1.	100.01	11.	100.00
2.	.06	12.	.04
3.	.03	13.	.01
4.	.02	14.	.07
5.	.02	15.	.02
6.	.05	16.	.02
7.	.04	17.	.03
8.	.03	18.	.02
9.	.00	19.	.03
10.	.06	20.	.05

Standard Deviation
σ = 0.017

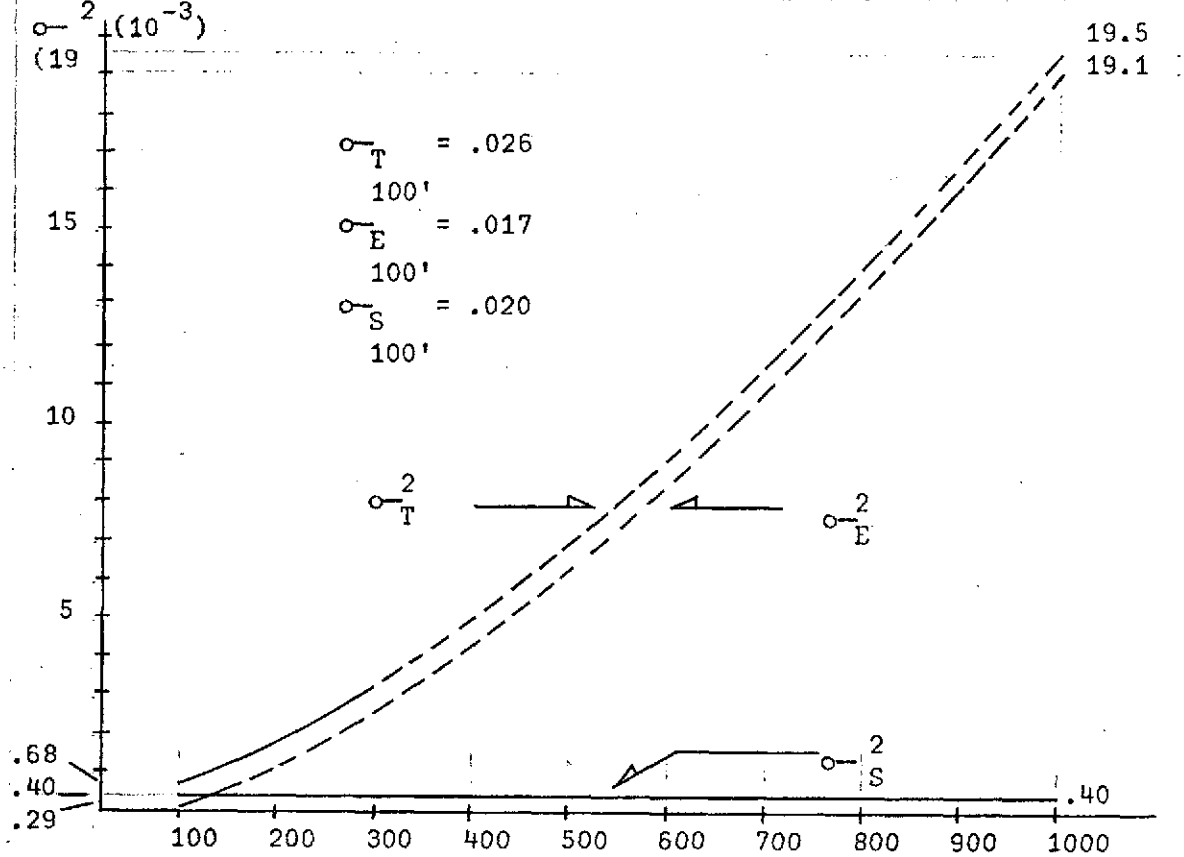

Figure 34. Standard Deviation Squared

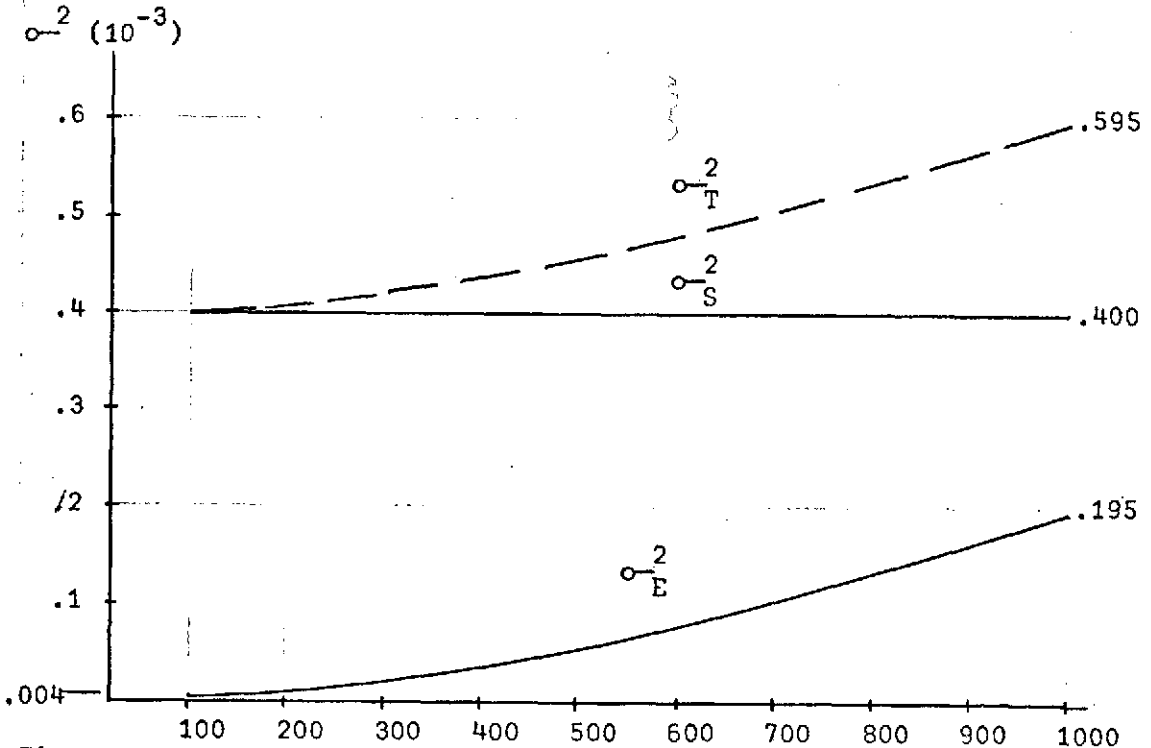

Figure 35. Standard Deviation Squared of Modified System

not exceed 0.03, it is obvious that the system will only measure with this accuracy up to about 150'; however, if enough measurements are made, the system can produce second order accuracies.

In order to investigate this, consider the standard deviation of the new parameter $s = \sigma/(n)^{\frac{1}{2}}$, where s is the standard deviation of the mean and n is the number of readings. For second order, $s_{max} = L/15{,}000$ where L is the distance measured and 15,000 is the quanity defining the second order accuracy. With thirty measurements, Table III gives the standard deviation of the mean for 5 distances measured and the 1000' conjucture.

TABLE III

STANDARD DEVIATION OF THE MEAN

Distance	σ	s	s(maximum)
100'	.026	.0047	.0067
150'	.031	.0057	.0100
200'	.043	.0078	.0133
250'	.049	.0110	.0167
300'	.054	.0121	.0200
1000'	.140	.0312	.0667

It is therefore seen that with thirty measurements taken, the system falls well within the second order requirements. However, thirty measurements takes around 20 minutes to record, which is too much time; so let us investigate just how many measurements are needed to obtain the second order accuracy and no more.

Table IV presents the values of σ and s for the number of measurements necessary to keep s less than or equal to s_{max}.

TABLE IV

STANDARD DEVIATION OF THE MEAN (n minimized)

Distance	$\sigma_{\bar{x}}$	n	s	s(maximum)
100'	.026	16	.0065	.0067
150'	.036	13	.0100	.0100
200'	.046	13	.0130	.0133
250'	.049	10	.0156	.0167
300'	.062	10	.0196	.0200

From the table, the maximum number of measurements that need be taken is 16, the average being 12. Hence, with the circuit design presently employed, if one takes 12 readings and then averages them, the reading will be of second order accuracy. This averaging procedure is justified because the nature of the error is random and will average out if enough readings are taken.

A significant improvement in the circuit could be incorporated into the design by replacing the 3-counter D/A by a 4-counter D/A (with a ten-fold unit increase in cost from $25 to $250), this would improve the accuracy of the electronics by a factor of ten--from 1 part per 1000 at 100' to 1 part per 10,000; and, from 1 part per 100 at 1000' to 1 part per 1000. The net effect would be as shown by figures 35 and 36. In figure 35, the total standard deviation squared is the sum of $\sigma_{\bar{x}_S}$ and $\sigma_{\bar{x}_E}$ (dotted line), where the new standard deviation squared of the electronics is 1/100 of the old.

The addition of the 4-counter D/A would make the system much more accurate. It would also make the servomotor variation and misalignment of the photodiodes to become the limiting factor in the system error because the standard deviation due to the electronics would drop below the value due to the electronics. This is assuming that the limit of resolution of the Hybrid-Optiverter was not exceeded. This aspect of the opti-

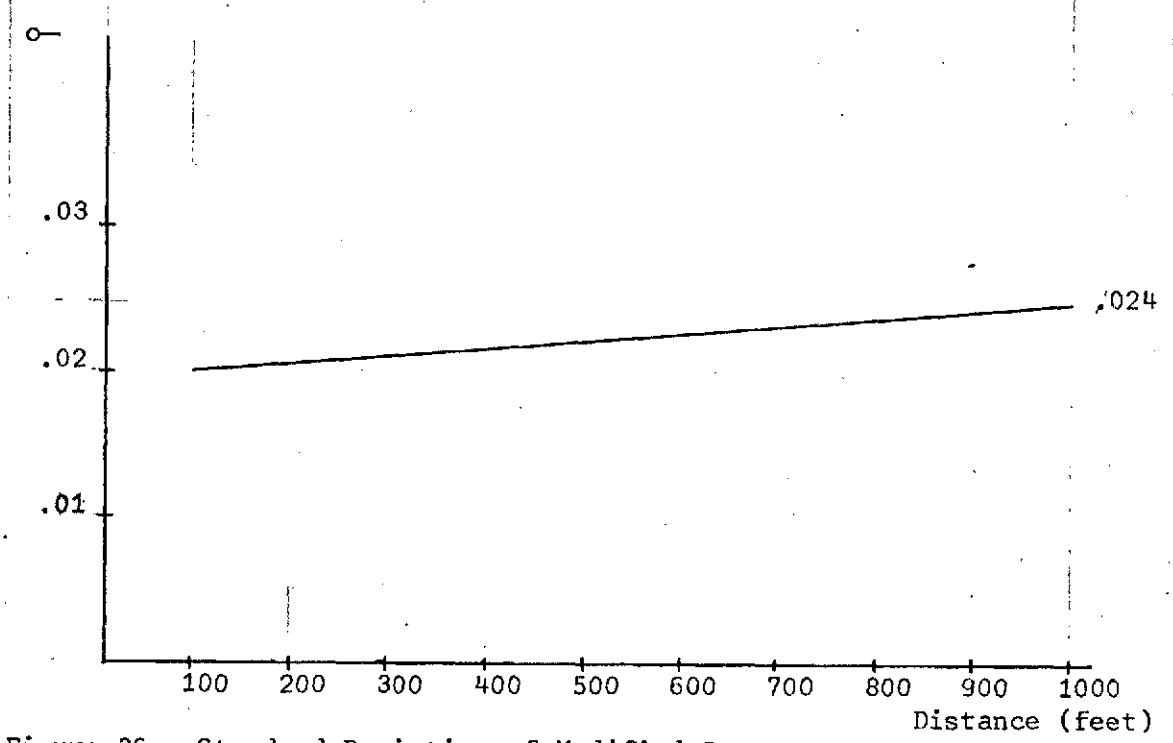

Figure 36. Standard Deviation of Modified System

verter remains to be investigated, however, it might be stated, that in order to get this resolution the clock rate supplied to the Optiverter would have to be increased, and the highest quality components associated with the unit be used. The constant source of current would have to be constant to at least 1 part per 10,000. Also, the assumed standard deviation of the sweeper would most probably differ from that given and would certainly have to be investigated. Again, alignment errors would also appear as being significant.

Another aspect of the system which could possibly improve its performance and cost would be to replace the servomotor with a tauntband optical scanner.

As a final note the dual photodetector system used could be replaced by a single photodiode with a mirror arrangment. The orginal design with two separate units was used to assure absolute separation of the signals; however, as the design proceeded and the system time parameters established, it is considered that the worst case 1 msec pulse separation is sufficient to allow the receiving system to recover its initial conditions regardless of possible states of saturation of the various components.

Cost Analysis

The system could be designed to mount on existing equipment already owned by the surveyer. Therefore the major cost lies in the components themselves. A rough estimate of the value of these is as follows:

1	Photodiode	$ 40
1	Optical Filter	65
1	4-Counter D/A	250
25	IC Chips	40
14	Transistors	10
1	5 Digit LED Readout	60
1	Laser	250
	Miscellaneous	100

The total cost for one unit would be $815.

Conclusion

Through the design and construction of the short-range distance measuring instrument, it has been shown that the accuracies required can be achieved by taking a series of measurements and averaging them. A circuit modification consisting of replacing the 3-counter D/A by a 4-counter D/A would substantially reduce the system errors producing a convenient effective low cost instrument of the desired accuracy.

REFERENCES

1. "Silicon Photodetector Design Manual", Publication by United Detector Technology. 1732 21st Street, Santa Monica, Calif.
2. Born & Wolf, Principles of Optics, London, Pergamon Press, 1965,p.396.
3. Sears & Zamansky, University Physics, Mass., Addison-Wesley, 1964, p. 875.
4. Ross, Laser Receivers, New York, John Wiley & Sons, 1966, p.61.
5. American Congress on Surveying and Mapping
6. Arfken, Mathematical Methods for Physicists, New York, Academic Press, 1966, p. 377.